MCB
Journals.ASM.org

C/EBPγ Suppresses Senescence and Inflammatory Gene Expression by Heterodimerizing with C/EBPβ

Christopher J. Huggins,[a] Radek Malik,[a]* Sook Lee,[a] Jacqueline Salotti,[a] Sara Thomas,[a] Nancy Martin,[a] Octavio A. Quiñones,[b] W. Gregory Alvord,[b] Mary E. Olanich,[a]* Jonathan R. Keller,[a] Peter F. Johnson[a]

Laboratory of Cancer Prevention, Center for Cancer Research, NCI—Frederick, Frederick, Maryland, USA[a]; DMS, Inc., Frederick National Laboratory for Cancer Research, Frederick, Maryland, USA[b]

C/EBPβ is an important regulator of oncogene-induced senescence (OIS). Here, we show that C/EBPγ, a heterodimeric partner of C/EBPβ whose biological functions are not well understood, inhibits cellular senescence. *Cebpg*$^{-/-}$ mouse embryonic fibroblasts (MEFs) proliferated poorly, entered senescence prematurely, and expressed a proinflammatory gene signature, including elevated levels of senescence-associated secretory phenotype (SASP) genes whose induction by oncogenic stress requires C/EBPβ. The senescence-suppressing activity of C/EBPγ required its ability to heterodimerize with C/EBPβ. Covalently linked C/EBPβ homodimers (β∼β) inhibited the proliferation and tumorigenicity of Ras^{V12}-transformed NIH 3T3 cells, activated SASP gene expression, and recruited the CBP coactivator in a Ras-dependent manner, whereas γ∼β heterodimers lacked these capabilities and efficiently rescued proliferation of *Cebpg*$^{-/-}$ MEFs. C/EBPβ depletion partially restored growth of C/EBPγ-deficient cells, indicating that the increased levels of C/EBPβ homodimers in *Cebpg*$^{-/-}$ MEFs inhibit proliferation. The proliferative functions of C/EBPγ are not restricted to fibroblasts, as hematopoietic progenitors from *Cebpg*$^{-/-}$ bone marrow also displayed impaired growth. Furthermore, high *CEBPG* expression correlated with poorer clinical prognoses in several human cancers, and C/EBPγ depletion decreased proliferation and induced senescence in lung tumor cells. Our findings demonstrate that C/EBPγ neutralizes the cytostatic activity of C/EBPβ through heterodimerization, which prevents senescence and suppresses basal transcription of SASP genes.

Cellular senescence is an irreversible state of cell cycle arrest induced by a variety of stimuli, including DNA damaging agents and activated oncogenes, which have the potential to cause neoplastic transformation (1, 2). Senescence, like apoptosis, provides a first-line defense against oncogenic threats and represents a key barrier to cancer development (3). Senescent cells typically display a flattened morphology, increased vacuolization, and induction of specific molecular markers, such as senescence-associated β-galactosidase (SA–β-Gal), as well as expression of the tumor suppressors p16^{Ink4a}, p19^{Arf}, and p53. Cells that lack these tumor suppressors are able to bypass senescence and, consequently, can be transformed by activated *ras* or other oncogenes.

Senescent cells remain metabolically active and secrete a cocktail of inflammatory cytokines, chemokines, and growth factors, collectively termed the senescence-associated secretory phenotype (SASP) (4). These factors are thought to identify senescent cells to the immune system, acting as signals for clearance of damaged or precancerous cells. In support of this model, Kang et al. (5) recently reported that "senescence surveillance" by a T-cell-mediated adaptive immune response is required for efficient suppression of oncogenic N-*ras*-induced liver tumorigenesis in mice through removal of premalignant cells. These findings provide compelling evidence for SASP-directed immune clearance of incipient tumor cells. SASP cytokines and chemokines also act on the senescing cells themselves via paracrine/autocrine signaling to reinforce the senescence program. This conclusion is based on studies showing that loss of the inflammatory mediators interleukin 6 (IL-6) and IL-8, or their receptors, prevents cells from undergoing replicative and oncogene-induced senescence (OIS) (6, 7). Thus, secreted inflammatory mediators play important roles in establishing the senescent state as well as communicating with the immune system to facilitate elimination of damaged cells.

Due to the irreversible nature of senescence and the deleterious effects of chronic production of inflammatory mediators, including their ability to establish a protumorigenic environment, senescence and SASP gene expression must be tightly controlled. NF-κB and C/EBPβ are inducible transcription factors that regulate SASP gene transcription (6–10). Genetic studies and RNA interference (RNAi) experiments have also demonstrated that C/EBPβ is required for OIS in human and murine fibroblasts (7, 11). C/EBPβ dimerizes with the small C/EBP family member, C/EBPγ, and C/EBPβ:C/EBPγ heterodimers are the predominant C/EBP DNA-binding species in a broad spectrum of cell types (12). C/EBPγ lacks a transactivation domain but contains a C/EBP-like bZIP region and can inhibit transcription by C/EBP activator proteins in reporter assays through heterodimerization (12–14). Moreover, the formation of C/EBPβ homodimers is stimulated by oncogenic Ras signaling through p90^{RSK}-mediated phosphorylation of a conserved leucine zipper residue, Ser273,

Received 12 December 2012 **Returned for modification** 3 January 2013
Accepted 6 June 2013
Published ahead of print 17 June 2013

Address correspondence to Peter F. Johnson, johnsope@mail.nih.gov.

* Present address: Radek Malik, Institute of Molecular Genetics, Academy of Sciences of the Czech Republic, Videnska, Prague, Czech Republic; Mary E. Olanich, Laboratory of Pathology, National Cancer Institute, Bethesda, Maryland, USA.

C.J.H., R.M., and S.L. contributed equally to this work.

Supplemental material for this article may be found at http://dx.doi.org/10.1128/MCB.01674-12.

doi:10.1128/MCB.01674-12

which controls self-dimerization by increasing the electrostatic interactions between paired leucine zipper helices (15). Based on these and other considerations, we have proposed that Ras-induced C/EBPβ homodimers are cytostatic and promote cell cycle arrest and senescence in response to oncogenic stress (8, 15).

The prevalence of C/EBPβ:C/EBPγ heterodimers in many cell types suggests that C/EBPγ has an important role in modulating C/EBPβ activity. Since β:γ heterodimers display reduced transcriptional potential, we hypothesized that C/EBPγ may inhibit the senescence-inducing activity of C/EBPβ. Here, we have analyzed *Cebpg*$^{-/-}$ mouse embryonic fibroblasts (MEFs) to investigate the biological functions of C/EBPγ. In contrast to C/EBPβ-deficient MEFs, which show enhanced growth, *Cebpg*$^{-/-}$ cells display impaired proliferation, increased spontaneous senescence, and elevated levels of proinflammatory cytokines. The proliferative defect in *Cebpg*$^{-/-}$ cells was partially abrogated by reducing C/EBPβ levels. β:β homodimers were increased in *Cebpg*$^{-/-}$ MEFs, and several lines of evidence indicate that homodimers activate SASP genes, whereas β:γ heterodimers lack this ability. In addition, hematopoietic progenitors from *Cebpg*$^{-/-}$ mouse bone marrow display proliferative defects, and high levels of *CEBPG* were associated with increased mortality or relapse in several human cancers. Our findings provide the first evidence that C/EBPγ acts as a negative regulator of senescence and promotes proliferation of multiple cell types.

MATERIALS AND METHODS

Mouse strains and preparation of MEFs. Animals were maintained in accordance with National Institutes of Health animal guidelines. C57BL/6 *Cebpg*$^{+/-}$ mice were kindly provided by Tsuneyasu Kaisho (16). The strain was continuously backcrossed to wild-type (WT) C57BL/6 mice to maintain the stock or backcrossed to WT 129Sv animals for 10 generations to obtain pure 129Sv *Cebpg*$^{+/-}$ mice. C57BL/6 *Cebpg*$^{+/-}$ mice were intercrossed to obtained embryos representing all three *Cebpg* genotypes on a pure C57BL/6 background. Alternatively, C57BL/6 *Cebpg*$^{+/-}$ animals were mated to 129Sv *Cebpg*$^{+/-}$ mice to create F1 hybrid progeny; homozygous mutant mice survived to adulthood on this mixed-strain background. To generate double-knockout embryos, C57BL/6 *Cebpg*$^{+/-}$ animals were mated to C57BL/6 *Cebpb*$^{+/-}$ animals, and F1 progenies heterozygous for both loci were intercrossed to generate compound mutant progenies. MEFs were prepared from embryonic day 13.5 (E13.5) embryos of the appropriate genotypes, and cells were cultured in Dulbecco's modified Eagle's medium (DMEM) (Invitrogen) supplemented with 10% fetal bovine serum (FBS; Gibco) and 100 U/ml penicillin-streptomycin (Gibco).

Cells and cell culture. NIH 3T3 cells were maintained in DMEM supplemented with 10% calf serum (Colorado Serum Company). MEFs, L929 fibroblast cells, HEK293T cells, A549 cells, GP2 cells (provided by S. Hughes), and Phoenix ecotropic packaging cells (provided by H. Young) were cultured in DMEM supplemented with 10% FBS (Gibco). All media included 100 U/ml penicillin-streptomycin (Gibco).

Plasmids. Tethered dimer constructs (17) were generated by joining hemagglutinin (HA)-tagged mC/EBPβ or mC/EBPγ sequences with the appropriate dimeric partner via a leucine-glutamic acid linker to produce single-chain γ∼γ, γ∼β, and β∼β dimers. The internal methionine residue in the mC/EBPβ monomer was mutated to alanine using site-directed mutagenesis (Stratagene) to eliminate translation of the truncated liver inhibitory protein (LIP) isoform. All constructs were cloned into pcDNA3.1 and pBabe-puro expression vectors.

Retroviral vectors and viral infection. pBabe-puro vector was kindly provided by S. Lowe. Mouse C/EBPγ, mC/EBPγ-G_{LZ}, which contains a swapped leucine zipper domain from GCN4 (18), mC/EBPβ and its LIP isoform (11), human papillomavirus (HPV)-derived E7, human cyclin D1, and chicken c-Myc (provided by P. Kaldis) were constructed and transferred to pBabe-puro. Human H-Ras^{V12} was expressed from pWZL-hygro (11). Knockdown small hairpin RNA (shRNA) sequences against mC/EBPβ and hC/EBPγ were generated and inserted into pSuper-Retro (Oligogene). Mouse Cebpb1 and Cebpb2 shRNAs were based on previously reported sequences (19, 20). We designed two hC/EBPγ shRNAs, CEBPG1 (GCAACGCCGAGAGAGGAAC) and CEBPG2 (GACCCATTG GAGGCTATTT), the latter with the aid of RNA structure prediction software (21). Retroviral plasmids were transfected into either Phoenix ecotropic or GP2 amphotropic packaging cells using standard $CaPO_4$ precipitation. A total of 24 to 72 h after transfection, viral supernatants were collected every 12 h, pooled, filtered (0.45-μm pore size), supplemented with 8 μg/ml Polybrene, and used to infect target cells. Four infections were performed, and the cells were selected for 3 days in 2 μg/ml puromycin or 200 μg/ml hygromycin. Multiple genes were introduced by sequential infection and drug selection.

Transient transfection. Transfections were carried out using 50 to 60% confluent cell monolayers in 10-cm dishes or 6-well plates using FuGENE6 (Roche). For all experiments, the total amount of DNA (1.5 μg per 6-well plate) was kept constant by adding an appropriate amount of pBluescript plasmid. Culture media were changed 24 h posttransfection, and cells were harvested 48 h after transfection.

Cell proliferation assays. For 3T3 proliferation experiments, MEFs were maintained on a 3-day serial passaging protocol (22). Cells (3×10^5) were plated in 10-cm dishes, and 3 days later the cell number was determined and 3×10^5 cells were replated. Growth curves on retrovirally infected MEFs and NIH 3T3^{RasV12} cells (passages 1 to 3) were seeded at 2.5×10^4 cells/well in six-well plates (in triplicate). At the indicated times, cells were washed with phosphate-buffered saline (PBS), fixed in 10% formalin, rinsed with water, stained with 0.1% crystal violet (Sigma) for 30 min, rinsed extensively, and dried. The dye was extracted with 10% acetic acid, and absorbance was measured at 590 nm. All values were normalized to day 0 (the first day after plating the cells), and assays were done in duplicate. For colony assays, MEFs (passages 2 to 4) were seeded at a density of 2.5×10^4 cells/100-mm plate. After 14 days, plates were washed with PBS, fixed in 10% acetic acid, rinsed with water, and stained with 0.4% crystal violet for 45 min. Assays were conducted in duplicate.

Transformation assays. Focus formation and anchorage-independent growth assays were performed using retrovirally infected 3T3^{RasV12} cells expressing CEBPβ, CEBPγ, or tethered dimers. For focus formation assays, 100 cells from infected 3T3^{RasV12} populations were plated in 100-mm dishes with 3.5×10^5 normal NIH 3T3 cells, and foci were counted after 14 days. For soft agar assays, 250 cells from infected samples were mixed in 0.35% agar-DMEM and overlaid on a 0.7% agar-DMEM base in a 60-mm dish. Colonies were counted after 14 days. All experiments were performed in triplicate.

Immunoblotting. Whole-cell lysates were prepared as described previously (23). Cells were lysed in buffer A (PBS [pH 7], 10% glycerol, 0.5 mM EDTA, 1 mM dithiothreitol [DTT], 2 mM NaF, 0.2% Triton X-100) for 15 min at 4°C. Lysates were cleared by high-speed centrifugation for 20 min at 18,000 × *g* at 4°C. Nuclear extracts were prepared as described previously (24). Briefly, cells were washed with PBS, scraped, resuspended in lysis buffer (20 mM HEPES [pH 7.9], 1 mM EDTA, 10 mM NaCl, 1 mM DTT, 0.1% Nonidet P-40, 0.5 mM phenylmethylsulfonyl fluoride) and incubated on ice for 10 min. Nuclei were pelleted by centrifugation at 3,500 rpm for 10 min. Proteins were extracted from nuclei by incubation in high-salt buffer (25 mM HEPES [pH 7.9], 0.2 mM EDTA, 0.42 M NaCl, 0.2 mM DTT, 25% glycerol, 0.5 mM phenylmethylsulfonyl fluoride) at 4°C for 20 min with vigorous shaking. Nuclear debris was pelleted by centrifugation at 14,000 rpm for 5 min, and the supernatant was used for further experiments or stored at −70°C. All buffers used were supplemented with protease inhibitors (Roche). Protein concentrations were determined using the Bradford protein assay (Bio-Rad).

A 25- to 30-μg sample of nuclear extract or 50 to 80 μg of whole-cell lysate was resolved by 12% SDS-PAGE and blotted to polyvinylidene di-

fluoride (PVDF) membranes (Millipore). Primary antibodies were as follows: C/EBPβ (C-19; Santa Cruz), C/EBPγ C-terminal (12), p53 (CM5; Novacastra), cyclin A (C-19; Santa Cruz), E2F-1 (KH-95; Santa Cruz), p21 (C-19; Santa Cruz), cyclin D1 (A-12; Santa Cruz), p15 (K-18; Santa Cruz), p16 (M-156; Santa Cruz), p18 (N-20; Santa Cruz), $p19^{Arf}$ (ab80; Abcam), HA tag (Y-11; Santa Cruz), and β-actin (C-11; Santa Cruz) antibodies. Antibodies against cyclin B, cyclin E1, cdk1, ckd2, cdk4, and cdk6 were kindly provided by P. Kaldis (23). Secondary antibodies conjugated to horseradish peroxidase were used to detect antigen-antibody complexes by using a chemiluminescent ECL detection system (Pierce).

EMSA. Electrophoretic mobility shift assay (EMSA) was performed as described previously (12). A probe containing the consensus C/EBP site was end-labeled using [^{32}P]dATP (Amersham) and polynucleotidyl kinase (Roche). DNA-binding assays were carried out in a 25-μl reaction mixture containing 20 mM HEPES (pH 7.9), 200 mM NaCl, 5% Ficoll, 1 mM EDTA, 50 mM DTT, 0.01% Nonidet P-40, 1.75 μg poly(dI-dC), and 2×10^4 cpm probe. After incubation for 20 min at room temperature, 10 to 15 μl of the binding reaction was loaded onto a 6% polyacrylamide gel in TBE (90 mM Tris base, 90 mM boric acid, 0.5 mM EDTA) buffer and electrophoresed at 160 V for 2 h. Supershift assays were carried out by preincubating the nuclear extract with 1 μl of the appropriate antibody at 4°C for 30 min before the addition of the binding reaction mixture.

Flow cytometry. L929 cells and HepG2 cells were transiently transfected with 0.5 μg CD20 expression vector and either 1.5 μg of C/EBPβ, 1.5 μg C/EBPβ and 5 μg C/EBPγ, or 5 μg C/EBPγ. The cells were harvested 48 h posttransfection, washed in PBS, incubated with CD20-fluorescein isothiocyanate (FITC) antibody (Becton, Dickinson; 347673), and fixed in 70% methanol for 2 h at 4°C. For flow cytometry, cells were resuspended in PBS and treated with 50 μg/ml of RNase A for 15 min followed by the addition of 50 μg/ml of propidium iodide. Samples were analyzed on a FACSCalibur cell sorter (Becton, Dickinson), and cells were measured for fluorescein isothiocyanate fluorescence (green channel) and propidium iodide (red channel). Total cell populations were gated to remove doublet cells and small particles. Cells transfected with vector alone were used to assess the background level of green fluorescence. Cell cycle analysis was performed with CellQuest analysis software (Becton, Dickinson). The percentage of cells with G_1 or S/G_2 DNA content was calculated relative to the total transfected (CD20-positive) population.

BrdU incorporation and flow cytometry analysis of MEFs. The percentage of cells in S phase was measured in unsynchronized and synchronized MEFs by bromodeoxyuridine (BrdU; Sigma-Aldrich) incorporation. For synchronization, primary MEFs were cultured in low serum (0.1% FBS) for 60 h, and cell cycle entry was induced by transfer into medium containing 10% FBS. Cells were pulse-labeled with 100 μM BrdU for 45 min prior to the indicated time points and then harvested. Cells were washed with PBS, fixed with 70% ethanol overnight, stained with 1 μg of fluorescein-conjugated anti-BrdU antibody (Alexa Fluor 488–anti-BrdU monoclonal antibody PRB-1; Invitrogen), and then stained with propidium iodide (50 μg/ml; Sigma-Aldrich) containing RNase A (20 μg/ml; Sigma-Aldrich) for 15 min at room temperature. The samples were analyzed with a FACSCalibur cell sorter (Becton, Dickinson), and the data were processed using WinMDI software.

Microarray gene expression profiling. RNA for genome-wide expression analysis was prepared from WT and *Cebpg*$^{-/-}$ MEFs and from WT/Ras^{V12} and *Cebpb*$^{-/-}$/Ras^{V12} MEFs (RNeasy; Qiagen). RNAs from each isolate were used for independent microarray hybridization analysis (LMT/Affymetrix Group, SAIC—Frederick). Labeled cDNAs were hybridized to GeneChip mouse genome 430 2.0 arrays (Affymetrix). Detailed statistical methods are described below. Gene array data for NIH $3T3^{RasV12}$ and C/EBPβ-NIH $3T3^{RasV12}$ cells have been reported (8).

qPCR. RNA samples isolated from NIH 3T3 and MEF populations were used to determine expression levels of selected genes. cDNA was generated (reverse transcription kit; Qiagen) from total RNA, and quantitative PCR (qPCR) was performed using SYBR green with QuantiTect primers (Qiagen) and normalized against β-actin or β2-microglobulin. qPCR was performed using an Applied Biosystems 7500 real-time PCR system and SDS software (version 1.4) or a Bio-Rad CFX96 touch thermal cycler. Relative gene expression values were determined twice (in triplicate), and the data were averaged. Error bars represent standard errors of means (SEM). Student's *t* tests were utilized to determine *P* values.

CBP coimmunoprecipitation assays and ChIP. Pulldown assays of CBP binding to C/EBPβ were carried out as described previously (25). Chromatin immunoprecipitation (ChIP) assays were performed essentially as described previously (11). Briefly, subconfluent cell cultures (15-cm dish per ChIP reaction) were cross-linked with 1% formaldehyde for 10 min at 37°C, and the reaction was quenched with 0.125 M glycine. Cells were washed with PBS, resuspended in lysis buffer (0.1% SDS, 0.5% Triton X-100, 150 mM NaCl, 20 mM Tris-HCl, pH 8.1), and sonicated to obtain DNA fragments of ~500 to 1,000 bp. Immunoprecipitation was performed using 3 μg of anti-C/EBPβ antibody (C-19; Santa-Cruz), anti-C/EBPγ C-terminal antibody (12), or CBP antibody (ab2832; Abcam). Samples were immunoprecipitated with antibodies overnight at 4°C, and then protein A magnetic beads (New England BioLabs) were added and incubated for 30 min at 4°C. Precipitates were washed and processed for DNA purification. DNA was amplified by qPCR with sequence-specific primers using a Bio-Rad CFX96 touch thermal cycler. Primer sequences can be found in materials and methods in the supplemental material.

SA–β-Gal staining. WT and *Cebpg*$^{-/-}$ MEFs (passage 2 to 4) were plated at 7.5×10^4 or 1×10^5 cells per well in 6-well plates and cultured for 2 to 3 days. Cells were fixed and stained (senescence detection kit; Calbiochem) according to the manufacturer's instructions, except that the pH of the staining solution was adjusted below 6.0 with HCl to optimize senescence-associated β-galactosidase (SA–β-Gal) detection in mouse cells.

Bone marrow cell proliferation and CFU-c assays. Bone marrow cells harvested from WT, *Cebpg*$^{+/-}$, and *Cebpg*$^{-/-}$ mice were cultured in Iscove's modified Dulbecco's medium (IMDM) supplemented with 10% fetal bovine serum and human macrophage colony-stimulating factor (M-CSF; 100 ng/ml), human granulocyte colony-stimulating factor (G-CSF; 50 ng/ml), murine stem cell factor (SCF; 100 ng/ml), murine granulocyte-macrophage colony-stimulating factor (GM-CSF; 20 ng/ml), murine IL-3 (30 ng/ml), human thrombopoietin (TPO; 100 ng/ml), and human FLT-3L (100 ng/ml), as indicated. All growth factors were purchased from PeproTech. To evaluate proliferation, cells were labeled with EdU (Click-iT EdU kit; Invitrogen) according to the manufacturer's instructions. Incorporated EdU was analyzed by FACS-LSRII (BD Biosciences) and FlowJo software. For CFU-c assays, 1.5×10^4 cells were seeded in 35-mm dishes in semisolid agar medium supplemented as described above, and colonies were counted after 7 days.

Clinical lung adenocarcinoma gene expression data. *CEBPG* mRNA expression data from human cancer patients was obtained from the PrognoScan database (http://gibk21.bio.kyutech.ac.jp/mizuno/PrognoScan.org) (26).

Statistical analysis. Detailed analysis of genome-wide gene expression differences was carried out as described previously (8, 27, 28). Student's *t* test was used to determine *P* values of qPCR gene expression differences.

Microarray data accession number. Microarray data are deposited in GEO under accession number GSE47777.

RESULTS

C/EBPβ and C/EBPγ differentially affect cell proliferation. Because C/EBPβ can exert antiproliferative effects on several cell types (29), we investigated whether C/EBPγ also affects mitotic growth. Transfection experiments using murine L929 fibroblasts and human HepG2 hepatocarcinoma cells showed that ectopic C/EBPβ expression increased the number of G_1-phase cells and decreased the S/G_2 pool (Fig. 1A). In contrast, C/EBPγ did not appreciably affect the cell cycle. Coexpression of C/EBPγ reversed C/EBPβ-induced G_1 arrest to various degrees, possibly because β:γ heterodimers are formed that do not inhibit proliferation.

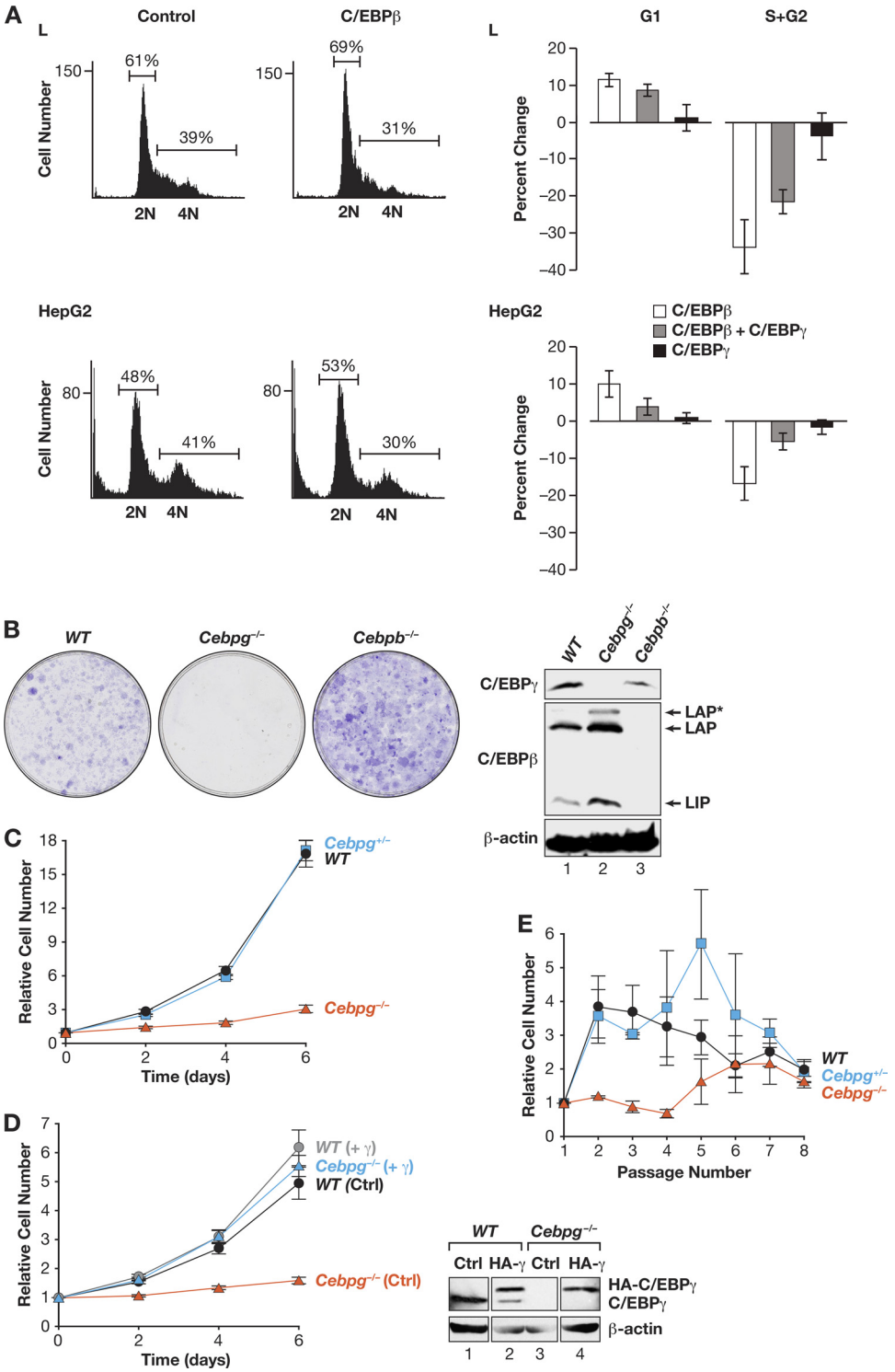

FIG 1 CEBPγ is required for efficient cellular proliferation. (A) Expression of C/EBPβ but not C/EBPγ increases G_1 arrest in HepG2 cells and L929 fibroblasts. Cells were transfected with CD20 expression vector and C/EBPβ, C/EBPγ, or C/EBPβ and C/EBPγ, harvested after 24 h, and stained with propidium iodide. CD20-positive cells were analyzed for DNA content. Graphs (left panels) show the effects of C/EBPβ overexpression. Average percent changes are shown on the right; data are mean values ± SEM from five experiments. (B) WT, *Cebpg*$^{-/-}$, and *Cebpb*$^{-/-}$ fibroblasts (MEFs) were isolated from E13.5 embryos and analyzed for colony growth. C/EBPβ and C/EBPγ protein levels were determined (right). Bands corresponding to the three C/EBPβ translational isoforms (LAP*, LAP, and LIP) are indicated. (C) Proliferation of WT, *Cebpg*$^{+/-}$, and *Cebpg*$^{-/-}$ MEFs was measured over 6 days. The data are mean values ± SEM from at least 10 independent MEF preparations, each assayed in triplicate. (D) Proliferation rates for WT and *Cebpg*$^{-/-}$ MEFs, without or with ectopic CEBPγ. The data are mean values ± SEM from at least 5 MEF isolates, assayed in triplicate. Right, C/EBPγ Western blot. Recombinant C/EBPγ is HA tagged and therefore migrates more slowly. (E) Long-term proliferative capacity of WT, *Cebpg*$^{+/-}$, and *Cebpg*$^{-/-}$ MEFs. Cells were propagated on a 3T3 protocol over 8 passages. The data are mean values ± SEM from 4 isolates of each genotype assayed in triplicate.

Thus, when overexpressed, C/EBPβ and C/EBPγ differentially affect cell cycle progression.

We next analyzed the proliferative potential of C/EBPγ-deficient MEFs. Clonogenic growth assays showed that low-passage-number *Cebpg*$^{-/-}$ cells formed few colonies and those that appeared were smaller than WT colonies (Fig. 1B). In contrast, *Cebpb*$^{-/-}$ cells exhibited increased clonogenicity compared to that of WT MEFs, consistent with previous data (11). WT and *Cebpg*$^{+/-}$ cells displayed similar proliferation rates, while *Cebpg*$^{-/-}$ MEF cultures grew much more slowly (Fig. 1C). Reexpression of ectopic C/EBPγ in *Cebpg*$^{-/-}$ MEFs restored normal proliferation (Fig. 1D); thus, loss of C/EBPγ does not lead to irreversible growth defects. Ectopic C/EBPγ had little effect on proliferation of WT MEFs, possibly because endogenous C/EBPγ levels are not limiting. In 3T3 passaging experiments, *Cebpg*$^{-/-}$ MEFs did not expand appreciably during the first several passages, whereas WT and heterozygous cells underwent many doublings (Fig. 1E). However, by passage 8, all three genotypes displayed equivalent proliferation rates (~1 cell doubling over 3 days), primarily because the expansion of WT and *Cebpg*$^{+/-}$ cells had slowed, indicating entry into replicative senescence. Collectively, these data demonstrate that C/EBPγ is required for efficient proliferation of MEFs.

***Cebpg*$^{-/-}$ MEFs display cell cycle defects.** To determine whether cell cycle progression is impaired in *Cebpg*$^{-/-}$ cells, we used BrdU incorporation to measure the number of S-phase cells in synchronized populations of WT and mutant MEFs at 18 h after serum stimulation (Fig. 2A). WT MEFs contained 39% BrdU^{Pos} cells at 18 h, whereas only 21% of *Cebpg*$^{-/-}$ MEFs were BrdU^{Pos}. BrdU incorporation assays performed over the time course showed that both WT and mutant cells began to enter S phase by 12 h. However, the percentage of BrdU^{Pos} *Cebpg*$^{-/-}$ cells was diminished at all times except 40 h, when the number of S-phase cells in the WT culture had declined significantly (Fig. 2B). Consistently, *Cebpg*$^{-/-}$ MEFs displayed a delayed and prolonged S phase, suggesting that C/EBPγ loss leads to defective progression through G_1/S. Accordingly, neutralization of Rb by the HPV E7 oncoprotein reversed the S phase defect, as did ectopic expression of C/EBPγ (Fig. 2C). Serum-induced levels of the cyclin-dependent kinases 1 (Cdk1), 2, 4, and 6 were nearly identical in WT and *Cebpg*$^{-/-}$ MEFs (Fig. 2D). However, cyclins D1, A, and E were reduced in mutant cells, while cyclin B levels were essentially unchanged. Although the Cdk inhibitor p27^{Kip1} was reproducibly increased in G_0 *Cebpg*$^{-/-}$ cells, degradation of the protein occurred efficiently following mitogen stimulation (30), indicating that the increased levels of p27^{Kip1} do not affect cell cycle progression. As p21^{CIP1} expression was modestly reduced in *Cebpg*$^{-/-}$ cells relative to WT MEFs, altered levels of p27^{Kip1} and p21^{CIP1} cannot account for the reduced proliferation of *Cebpg*$^{-/-}$ cells. We conclude that cell cycle progression is impaired in the absence of C/EBPγ and coincides with decreased expression of several cyclins.

We also tested the effects of overexpressing various cell cycle regulators on cell proliferation. HPV E7 enhanced the growth rate of *Cebpg*$^{-/-}$ cells (Fig. 2E), consistent with its effects on S-phase entry. Cyclin D1 and c-Myc, which are potent drivers of the cell cycle, also partially restored proliferation of *Cebpg*$^{-/-}$ cells, although not as effectively as ectopic C/EBPγ (Fig. 2F and G). Hence, the proliferative defects resulting from the absence of C/EBPγ cannot be explained solely by deficient cyclin D1 (or c-Myc) expression.

***Cebpg*$^{-/-}$ cells acquire a premature senescent phenotype.** *Cebpg*$^{-/-}$ MEF cultures contained many cells with a flattened morphology and vacuolated cytoplasm, indicative of premature entry into senescence (Fig. 3A). This observation was confirmed by SA–β-Gal staining assays, which showed that mutant MEFs contain ~4-fold more senescent cells than WT MEFs (Fig. 3B). Since senescence is often regulated by induction of the tumor suppressors p19^{Arf}, p16^{Ink4a}, p15^{Ink4b}, or other Ink4 family Cdk inhibitors, we compared their levels in WT and mutant cells at passages 2 to 4 (Fig. 3C). However, we observed no consistent increase in expression of these proteins or of p18^{Ink4c} in *Cebpg*$^{-/-}$ MEFs, indicating that induction of p19^{Arf} or Ink4 cell cycle inhibitors does not explain the enhanced senescence of mutant cells.

Identification of genes regulated oppositely by C/EBPβ and C/EBPγ that define an inflammatory signature. We previously showed that ectopic expression of C/EBPβ in NIH 3T3^{RasV12} cells inhibits proliferation and increases senescence (8). Moreover, gene expression profiling revealed elevated mRNA levels for several genes encoding SASP and other cytostatic proteins that are likely C/EBPβ targets. Since *Cebpg*$^{-/-}$ MEFs display a severe proliferation defect, we reasoned that genes overexpressed in the mutant cells may represent candidates for inducing growth arrest. In addition, these genes might be positively regulated by C/EBPβ, since C/EBPγ can inhibit C/EBPβ activity via heterodimerization. To compare the C/EBPβ transcriptome with genes repressed by C/EBPγ, we performed microarray studies using WT MEFs and cells lacking C/EBPγ or C/EBPβ. We anticipated that genes underrepresented in Ras^{V12}-expressing *Cebpb*$^{-/-}$ MEFs, which bypass OIS and proliferate more rapidly than WT cells (11), might identify additional antiproliferative genes that are presumptive C/EBPβ targets.

Array experiments were performed to elucidate gene expression differences between *Cebpg*$^{-/-}$ and WT MEFs and between *Cebpb*$^{-/-}$/Ras^{V12} and WT/Ras^{V12} MEFs. Based on these results and previous expression data from 3T3^{RasV12} cells (8), we generated gene lists defined by the following comparisons: $\geq +1.5$-fold expression difference ($P \leq 0.05$) for C/EBPβ-3T3^{RasV12} versus 3T3^{RasV12} cells and *Cebpg*$^{-/-}$ versus WT MEFs and ≤ -1.5-fold expression change ($P \leq 0.05$) for *Cebpb*$^{-/-}$/Ras^{V12} versus WT/Ras^{V12} MEFs (see Tables S1 and S2 in the supplemental material). The intersection of these three groups represents a subset of genes regulated by the C/EBPβ-C/EBPγ axis that may control growth arrest and senescence. We identified 47 genes that fulfilled these criteria (Fig. 4A, Venn diagram tri-intersect; for gene list, see Table S2). The 47-gene signature was analyzed using GeneGo Metacore software to identify associations with biological pathways and diseases; the 10 most significant correlations are listed in Fig. 4B. Seven of the 10 pathways were linked to immune responses and cytokine signaling, while the remaining 3 involved development, mucin expression, and liver fibrosis. Disease associations included pathologies such as inflammation, infections, and wounds/injuries. Notably, inflammation, liver fibrosis, and wound healing have all been linked to proliferative arrest and/or senescence (31–33).

Elevated basal SASP gene expression in *Cebpg*$^{-/-}$ cells. Since inflammatory genes were highly represented in the transcriptional profiles and C/EBPβ is implicated in SASP gene induction during OIS (7, 8, 10), we used qPCR to evaluate expression of candidate

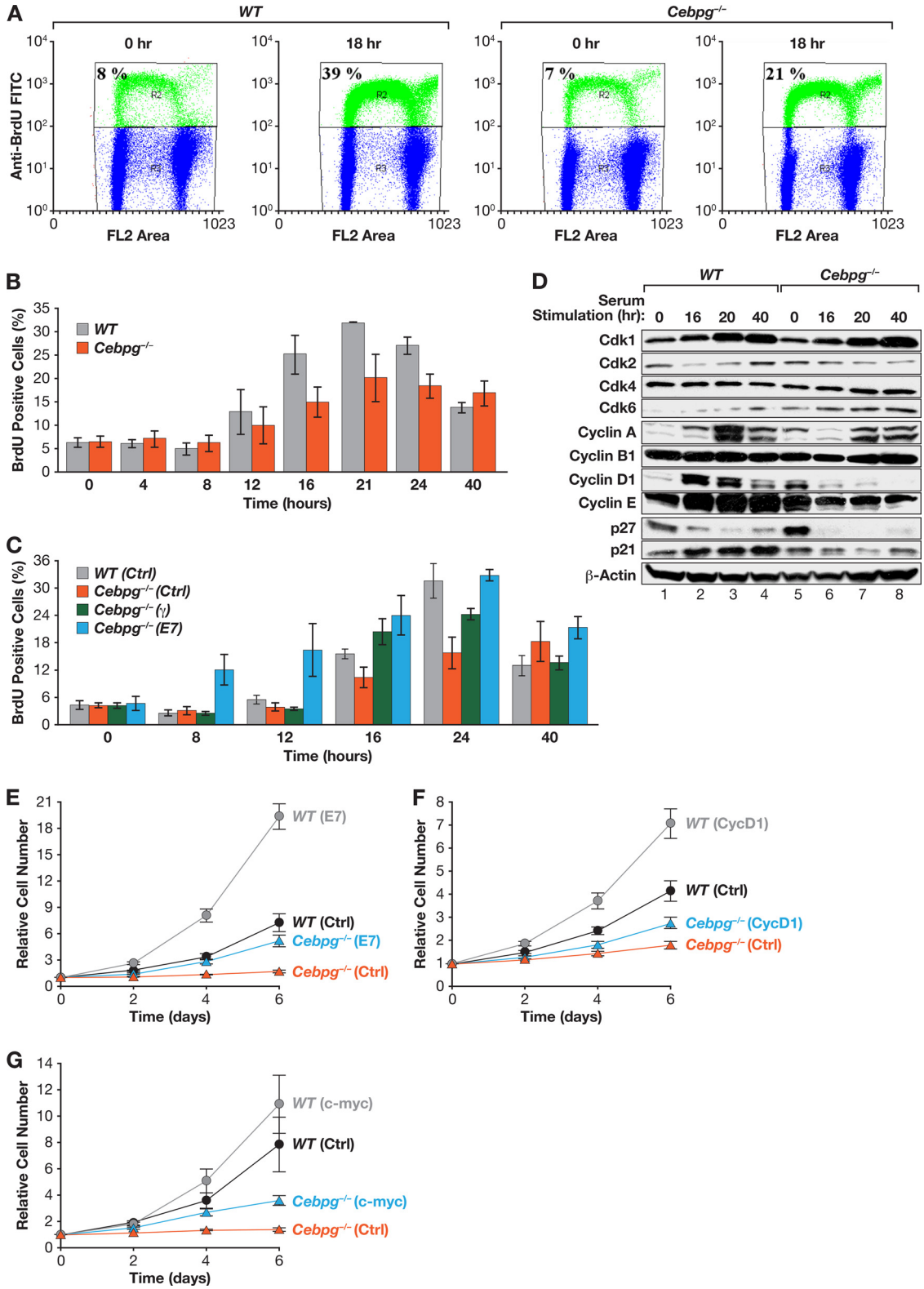

FIG 2 C/EBPγ is necessary for normal cell cycle progression. (A) WT and *Cebpg*$^{-/-}$ MEFs were synchronized by serum starvation, stimulated with serum, and labeled with BrdU. The percentage of cells in S phase after 18 h is shown. (B) Time course of cell cycle entry in WT and *Cebpg*$^{-/-}$ MEFs. Cells were serum starved, restimulated, and pulse-labeled with BrdU at the indicated times. Data are averages ± SEM from two experiments. (C) Expression of C/EBPγ or HPV oncoprotein E7 partially rescues delayed S-phase entry in *Cebpg*$^{-/-}$ MEFs. C/EBPγ and E7 were expressed in WT or *Cebpg*$^{-/-}$ MEFs, and the cells were analyzed as described above. Data are averages ± SEM from two experiments. (D) Cyclins D1, A, and E are reduced in *Cebpg*$^{-/-}$ MEFs. Lysates from serum-stimulated MEFs analyzed by Western blotting for CDKs (Cdk1/2/3/6), cyclins (A/B1/D1/E), and CDK inhibitors (p21/p27). (E to G) E7 and, to a lesser extent, cyclin D1 and c-Myc rescue growth of *Cebpg*$^{-/-}$ MEFs. WT and *Cebpg*$^{-/-}$ MEFs were transduced with vectors for E7 (E), cyclin D1 (F), or c-Myc (G) and proliferation was measured. Data are averages ± SEM from at least two experiments performed in triplicate.

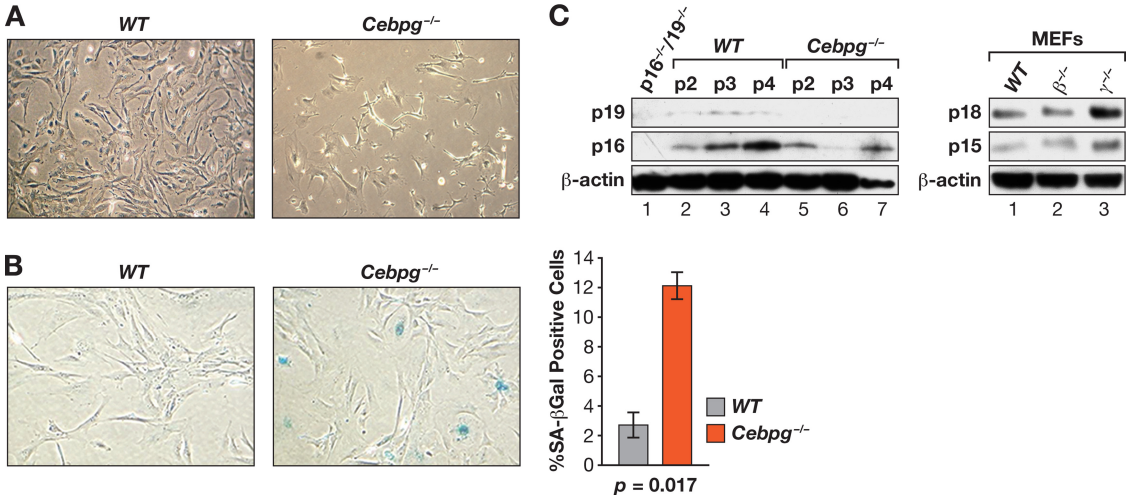

FIG 3 Increased senescence in *Cebpg*$^{-/-}$ MEFs. (A) Morphology of WT and *Cebpg*$^{-/-}$ cells 6 days after being plated. (B) Increased SA–β-Gal expression in *Cebpg*$^{-/-}$ MEFs. The frequency of SA–β-Gal-positive cells is shown. Data are the mean values ± SEM from 2 experiments. (C) Expression of cell cycle inhibitors in WT and *Cebpg*$^{-/-}$ MEFs. Left, p16^{Ink4a} and p19^{Arf} protein levels at passages 2 to 4. A lysate from *p16*$^{-/-}$/*p19*$^{-/-}$ MEFs is shown as a negative control (lane 1). Right, p15^{Ink4b} and p18^{Ink4c} protein levels in WT, *Cebpb*$^{-/-}$, and *Cebpg*$^{-/-}$ MEFs at passage 2. The apparent increase in p18^{Ink4c} expression in *Cebpg*$^{-/-}$ cells was not consistently observed.

SASP genes (*GROα/Cxcl-1*, *Cxcl2*, *Ccr-1*, *Il6*, *Il1a*, and *Il1b*) in *Cebpg*$^{-/-}$ MEFs and Ras^{V12}-expressing *Cebpb*$^{-/-}$ MEFs. Each gene was induced in C/EBPγ-deficient MEFs compared to WT cells; e.g., *GROα/Cxcl1* was enhanced by ~3.5-fold and *Il6* by ~2-fold (Fig. 4C). Furthermore, all of the SASP genes were strongly upregulated by Ras^{V12} in WT MEFs but not in *Cebpb*$^{-/-}$ cells (Fig. 4D). Thus, loss of C/EBPγ increases expression of SASP genes, while C/EBPβ is essential for their Ras^{V12}-induced activation. We also asked whether C/EBPγ deficiency caused increased expression of previously identified C/EBPβ target genes that are involved in cell cycle arrest and/or tumor suppression (8). Of this group, stefin A3 was upregulated ~5-fold in *Cebpg*$^{-/-}$ MEFs relative to WT cells, while the others (schlafen2, Btg2, p53 interacting protein 1, Vgll3, and thrombospondin 1 [Thbs1/TSP-1]) were unchanged (Fig. 4E). Collectively, these observations suggest that C/EBPγ suppresses basal transcription of SASP genes and other antiproliferative genes by inhibiting C/EBPβ.

C/EBPβ homodimers promote cell cycle arrest. Ras^{V12}-induced senescence in MEFs is correlated with increased C/EBPβ DNA binding and elevated levels of C/EBPβ homodimers (15), indicating that C/EBPβ homodimers regulate cell cycle arrest. Hence, the proliferation defects seen in *Cebpg*$^{-/-}$ MEFs could result from increased C/EBPβ homodimers. To address this possibility, we first performed EMSA and antibody supershifts to evaluate the C/EBP dimers in WT and *Cebpg*$^{-/-}$ cells (Fig. 5A). WT MEFs express a predominant C/EBPβ heterodimeric complex and a less abundant homodimeric form. The heterodimeric band consists of multiple species but was primarily supershifted by the C/EBPγ and C/EBPβ antibodies (lanes 2 and 3), indicating a preponderance of β:γ dimers. The identities of the complexes were further confirmed by comparison with proteins expressed in 293T cells (lanes 8 to 14). For example, overexpressed C/EBPβ (lane 8) comigrates with the upper band in MEFs identified as a C/EBPβ homodimer. Notably, *Cebpg*$^{-/-}$ cells showed significantly more C/EBPβ homodimers and less heterodimers than WT MEFs (compare lanes 1 and 5). Thus, levels of C/EBPβ homodimers are elevated in *Cebpg*$^{-/-}$ cells, similar to those in WT MEFs undergoing Ras-induced senescence (15).

These findings indicate that the proproliferative function of C/EBPγ involves its ability to heterodimerize with C/EBPβ. We therefore asked whether a heterodimerization-deficient C/EBPγ mutant bearing the GCN4 leucine zipper (C/EBPγ-G$_{LZ}$) (Fig. 5B) (18) could rescue growth of C/EBPγ-deficient cells. In contrast to C/EBPγ, C/EBPγ-G$_{LZ}$ was unable to stimulate proliferation of *Cebpg*$^{-/-}$ MEFs (Fig. 5C and D; see also Fig. 10E). Interestingly, LIP, a truncated translational isoform of C/EBPβ that contains a C/EBP bZIP domain but lacks a transactivation domain and is therefore structurally similar to C/EBPγ (Fig. 5B) (34), was also unable to substitute for C/EBPγ. In addition, C/EBPγ, but not C/EBPγ-G$_{LZ}$ or LIP, reversed the senescent phenotype of *Cebpg*$^{-/-}$ cells (Fig. 5E). We conclude that the ability of C/EBPγ to heterodimerize with C/EBPβ, and possibly other capabilities, such as dimerization with additional bZIP proteins, underlies its capacity to promote growth and suppress senescence.

Functional differences between C/EBPβ homodimers and β:γ heterodimers. To further elucidate the distinct activities of C/EBPβ homo- and heterodimers, we used a tethered dimer approach wherein two monomeric subunits are covalently joined by a flexible linker to force specific dimeric interactions (17). We generated covalent β~β, γ~β, and γ~γ dimers (Fig. 6A), which were initially expressed in 293T cells without or with Ras^{V12}, to assess DNA binding. EMSA showed that each protein bound efficiently to a C/EBP probe (Fig. 6B), demonstrating their ability to bind DNA. C/EBPβ analyzed in parallel (lanes 1 and 2) showed basal repression (autoinhibition) that was overcome by coexpression of Ras^{V12}, as observed previously (15). Interestingly, in contrast to native C/EBPβ, β~β dimers displayed strong basal DNA binding that was not further increased by Ras^{V12} (lanes 3 and 4); γ~β and γ~γ also showed high constitutive binding (lanes 5 to 8). This result suggests that the mechanism of C/EBPβ autoinhibition by N-terminal sequences (25) involves blocking dimeriza-

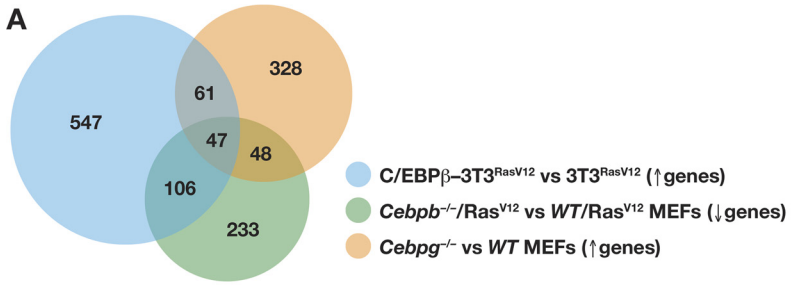

B

Pathway	*LOD Score*
Immune response_MIF-mediated glucocorticoid regulation	4.65
Immune response_IL-1 signaling pathway	3.73
Immune response_Histamine H1 receptor signaling in immune response	3.62
Mucin expression in CF via TLRs, EGFR signaling pathways	3.56
Immune response_HMGB1/RAGE signaling pathway	3.49
Immune response_TREM1 signaling pathway	3.35
Immune response_IL-17 signaling pathways	3.32
Immune response_Gastrin in inflammatory response	3.15
Stellate cells activation and liver fibrosis	3.12
Development_Glucocorticoid receptor signaling	2.77

Disease (by Biomarker)	*LOD Score*
Inflammation	9.47
Pathologic Processes	8.05
Pneumonia	7.42
Wounds and Injuries	7.21
Pathological Conditions, Signs and Symptoms	6.83
Carotid Artery Diseases	6.30
Cerebrovascular Disorders	6.05
Pulmonary Disease, Chronic Obstructive	5.79
Infection	5.37
Respiratory Tract Infections	5.27

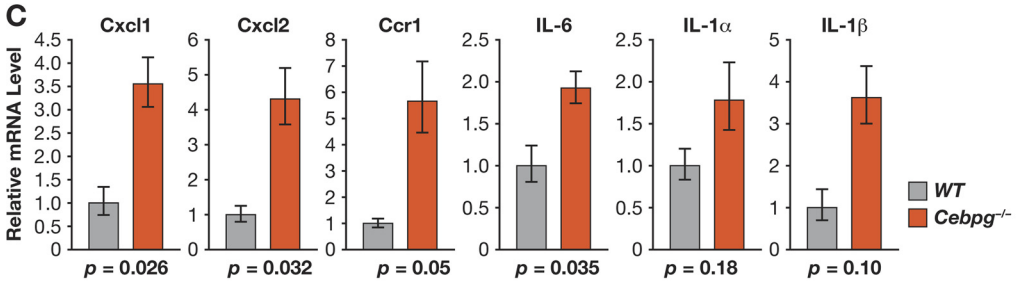

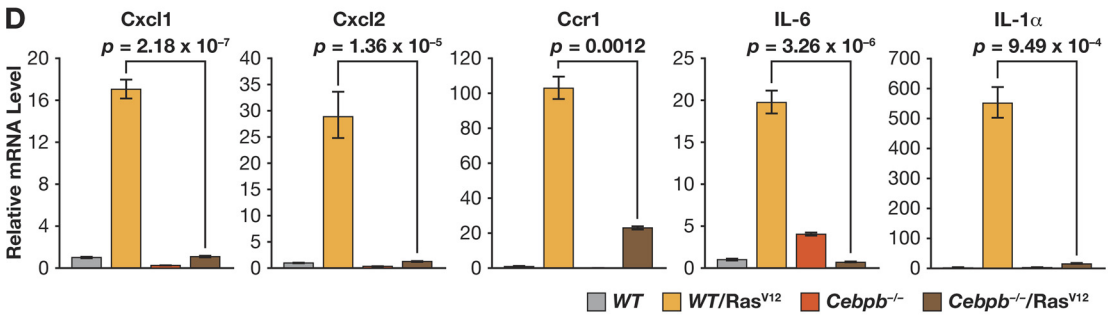

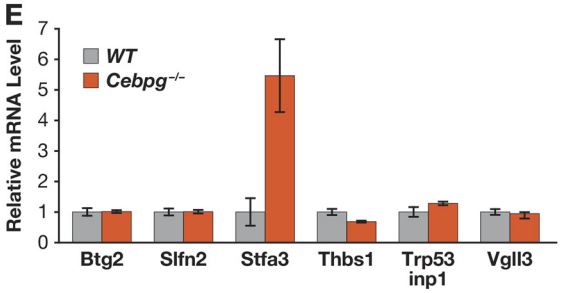

FIG 4 *Cebpg*$^{-/-}$ MEFs display a proinflammatory gene signature and enhanced expression of SASP genes. (A) Analysis of genes positively regulated by C/EBPβ and negatively regulated by C/EBPγ. Gene lists were generated from expression array comparisons: *Cebpg*$^{-/-}$ versus WT MEFs (increased expression; >+1.5-fold; $P < 0.05$), *Cebpb*$^{-/-}$/Ras^{V12} versus WT/Ras^{V12} MEFs (decreased expression; <−1.5-fold; $P = 0.05$), and C/EBPβ-3T3^{RasV12} cells versus 3T3^{RasV12} cells (increased expression; >+1.5-fold; $P < 0.05$). NIH 3T3 data are from Basu et al. (8). Venn diagram depicts the intersections of these groups. The triple intersect represents genes that are positively regulated by C/EBPβ and inhibited by C/EBPγ. (B) GeneGo pathway and disease associations of the tri-intersect gene set. (C) Expression of representative SASP genes in WT and *Cebpg*$^{-/-}$ MEFs. mRNA levels were determined by qPCR; data are mean values ± SEM from 2 triplicate measurements from 2 independent MEF isolates. (D) SASP gene expression is induced by oncogenic Ras^{V12} in WT but not *Cebpb*$^{-/-}$ MEFs. RNA isolated from control and Ras^{V12}-expressing MEFs was analyzed for SASP gene expression by qPCR. The data are mean values ± SEM from 2 triplicate measurements from 2 samples each. (E) Effect of C/EBPγ deficiency on expression of C/EBPβ target genes involved in tumor suppression or cell proliferation (8). The indicated genes were analyzed in WT and *Cebpg*$^{-/-}$ MEFs. Data are the means ± SEM from two experiments, assayed in triplicate.

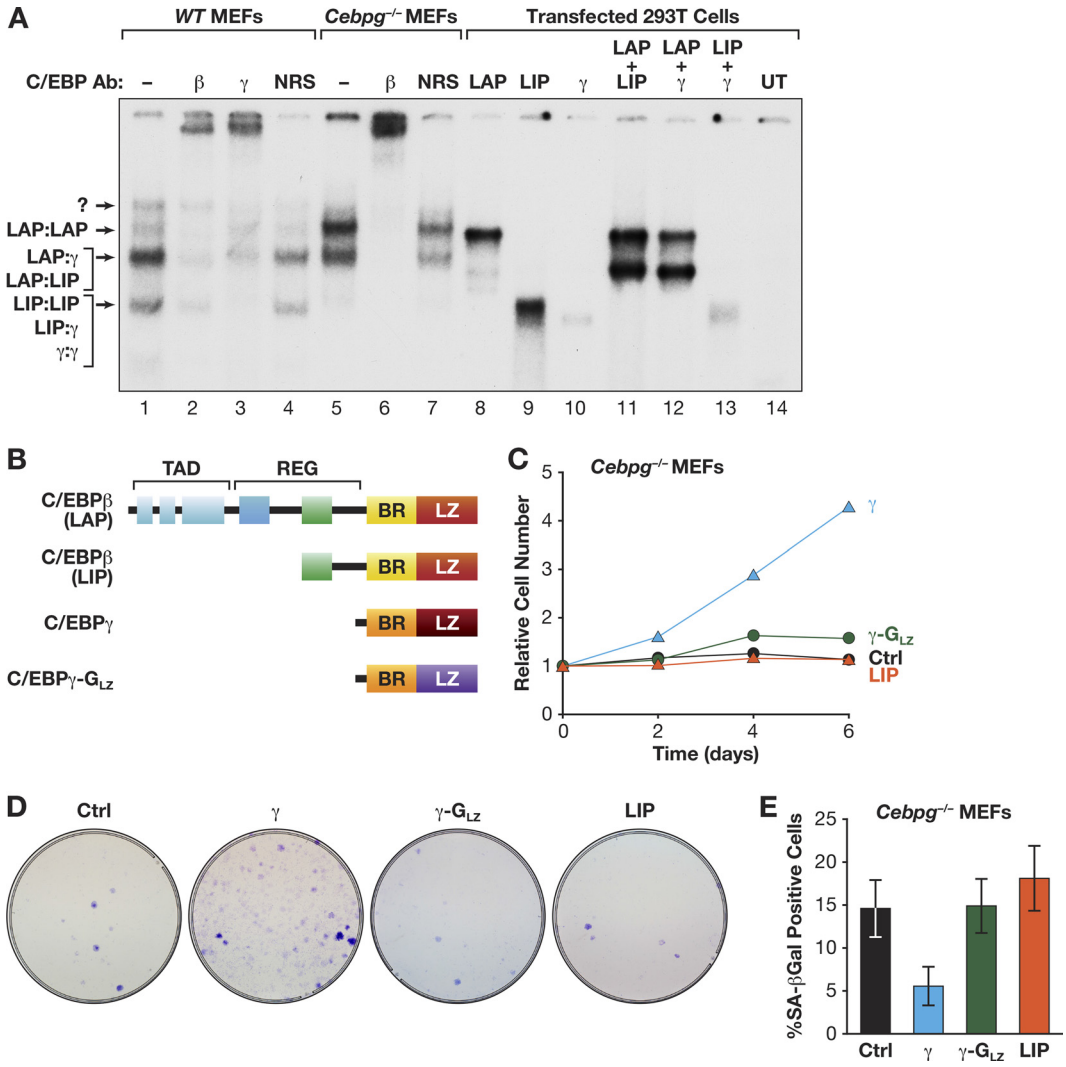

FIG 5 C/EBPγ stimulates cell proliferation by heterodimerizing with C/EBPβ. (A) EMSA was performed using a C/EBP consensus site probe and nuclear extracts from WT and *Cebpg*$^{-/-}$ MEFs (lanes 1 to 7). Antibody supershifts were performed to identify specific dimeric complexes. EMSAs were compared to those generated from cells overexpressing the indicated C/EBP proteins (lanes 8 to 14). The identities of C/EBP complexes are indicated. UT, untransfected cells; NRS, normal rabbit serum. (B) Domain structures of CEBPβ (LAP and LIP), C/EBPγ, and C/EBPγ-G_{LZ}. LAP is the major C/EBPβ isoform and is expressed from the second in-frame AUG codon; LIP is a truncated translational isoform (34). C/EBPγ-G_{LZ} contains the GCN4 leucine zipper. TAD, transactivation domain; REG, regulatory domain; BR, basic region; LZ, leucine zipper. (C) Proliferation assays of *Cebpg*$^{-/-}$ MEFs expressing C/EBPγ, LIP, or C/EBPγ-G_{LZ}. The data are mean values ± SEM from at least 4 experiments assayed in triplicate. (D) Colony assays. The cells described in the legend to panel C were plated at a density of 5×10^4 cells/dish and stained after 2 weeks. (E) The same populations were analyzed for senescent (SA–β-Gal-positive) cells (±standard deviation [SD]) from a representative experiment (>400 cells analyzed).

tion, which suppresses DNA binding in the absence of activating signals. Further studies are required to substantiate this model.

We next expressed β∼β, γ∼β, γ∼γ, or the individual subunits in *Cebpb*$^{-/-}$ MEFs to determine their effects on cell proliferation (Fig. 6C, left). C/EBPβ suppressed proliferation, as previously reported (11), and β∼β dimers also inhibited growth. In contrast, C/EBPγ and γ∼γ had no effect and γ∼β only partially inhibited proliferation. In Ras^{V12}-expressing *Cebpb*$^{-/-}$ MEFs, C/EBPβ and β∼β caused nearly complete arrest, while γ∼β had little effect and C/EBPγ and γ∼γ increased growth.

The same proteins were also tested in NIH 3T3 cells, where C/EBPβ-mediated growth arrest requires activation by Ras^{V12} signaling (35). None of the proteins showed appreciable cytostatic activity in normal 3T3 cells (data not shown). However, C/EBPβ and β∼β efficiently prevented growth of $3T3^{Ras}$ cells, while γ∼β had only a partial inhibitory effect and C/EBPγ and γ∼γ modestly stimulated proliferation (Fig. 7A). Furthermore, C/EBPβ and β∼β strongly suppressed focus formation and anchorage-independent growth of $3T3^{Ras}$ cells, while C/EBPγ, γ∼γ, and γ∼β had little effect, although γ∼β weakly inhibited growth in soft agar (Fig. 7B and C). We also used qPCR to assess a panel of C/EBPβ target genes in $3T3^{Ras}$ cells expressing each protein (Fig. 7D). C/EBPβ and β∼β efficiently induced expression of *Cxcl1*, *Cxcl2*, *Ccr1*, *Il6*, *Il1a*, and *Il1b*, whereas neither γ∼β, C/EBPγ, nor γ∼γ was capable of activating these genes. Collectively, Fig. 6 and 7 demonstrate that C/EBPβ homodimers induce cell cycle arrest and transcription of SASP genes, while β:γ dimers are permissive for growth and fail to activate inflammatory genes.

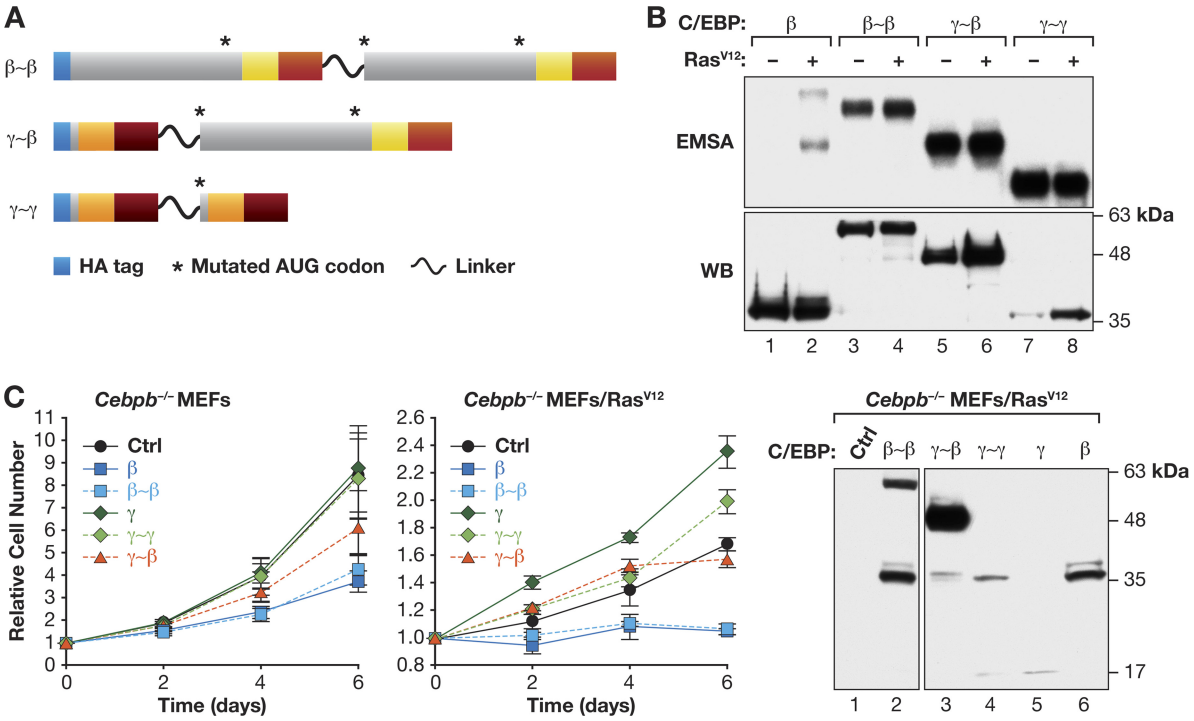

FIG 6 Opposing effects of C/EBPβ (LAP) homodimers and C/EBPγ:C/EBPβ heterodimers on cell proliferation. (A) Diagram of β~β, γ~β, and γ~γ tethered dimers. Proteins are HA tagged, and internal in-frame AUG codons were deleted. (B) DNA binding of tethered dimers. Proteins were expressed in 293T cells ± Ras^{V12} and cell extracts were subjected to EMSA. Protein levels were determined by HA Western blot. (C) Effects of linked dimers on proliferation of MEFs. *Cebpb*$^{-/-}$ or *Cebpb*$^{-/-}$/Ras^{V12} MEFs were infected with retroviruses encoding the indicated proteins, and cell proliferation was assayed. Data are the mean values ± SEM from 2 experiments assayed in triplicate. Right, C/EBP protein levels in transduced *Cebpb*$^{-/-}$/Ras^{V12} MEFs. The blot was probed with an HA antibody. The low levels of monomeric C/EBPβ and C/EBPγ in cells expressing tethered dimers result from partial proteolytic cleavage.

As C/EBPβ homodimers have much higher transcriptional activity than β:γ heterodimers, we investigated possible biochemical differences between these two complexes. C/EBPβ associates with p300/CBP coactivators in a manner that is strongly potentiated by Ras^{V12}, which also induces C/EBPβ homodimerization (25, 36). Therefore, we asked whether C/EBPβ homodimers and heterodimers bind differentially to CBP. A C-terminal segment of CBP containing the TAZ2 protein interaction domain was coexpressed with C/EBPβ, β~β, or γ~β in the absence or presence of Ras^{V12}, and pulldown assays were performed (Fig. 8A). C/EBPβ and β~β associated with CBP in a Ras-dependent manner, whereas γ~β exhibited no detectable binding to CBP, even when expressed with Ras^{V12}. These results indicate that homodimerization is necessary, but not sufficient, for C/EBPβ to associate with CBP. Apparently, additional Ras^{V12}-induced C/EBPβ modifications are required for homodimers to stably bind CBP.

We next used ChIP assays to assess binding of endogenous C/EBPβ, C/EBPγ, and CBP to the *Il6*, *Il1a*, and *Il1b* promoters, which contain known or predicted C/EBP sites (37) (see the supplemental material). We first compared binding in control and Ras^{V12}-expressing MEFs (Fig. 8B). In WT cells, C/EBPβ association with target promoters increased in response to oncogenic Ras, whereas C/EBPγ binding tended to decrease. These data are consistent with β:β and β:γ dimers binding to the same sites, with elevated levels of C/EBPβ homodimers in Ras-expressing cells causing displacement of β:γ heterodimers and enhancing transcription of SASP genes. Similarly, the absence of C/EBPγ in *Cebpg*$^{-/-}$ cells would lead to increased C/EBPβ homodimer occupancy of SASP promoters, stimulating transcription of these genes. Accordingly, we observed enhanced binding of C/EBPβ to the *Il6*, *Il1a*, and *Il1b* promoters in MEFs lacking C/EBPγ (Fig. 8C). CBP association with SASP gene promoters also tended to increase in Ras^{V12}-expressing cells in a manner that depends on C/EBPβ; indeed, CBP binding to the *Il6* and *Il1a* promoters was decreased by Ras in C/EBPβ-deficient cells (Fig. 8B and D). Furthermore, binding to the *Il6* promoter was enhanced in *Cebpg*$^{-/-}$ MEFs relative to that of WT cells (Fig. 8D).

C/EBPβ contributes to proliferation arrest in C/EBPγ-deficient cells. The data thus far indicate that C/EBPγ promotes cell proliferation through the ability to heterodimerize with C/EBPβ and inhibit its cytostatic activity. To directly test this hypothesis, we asked whether loss of C/EBPβ could partially or fully rescue the C/EBPγ-null phenotype. We intercrossed *Cebpg*$^{+/-}$; *Cebpb*$^{+/-}$ mice and isolated MEFs from the resulting E13.5 embryos. We obtained embryos representing each of the nine possible *Cebpg*; *Cebpb* genotypes, demonstrating that double-knockout animals remained viable at this stage. Analysis of the mutant MEFs showed that cells with any of the six *Cebpg*$^{+/+}$ or *Cebpg*$^{+/-}$ genotypes displayed similar proliferation rates, with only minor differences observed (Fig. 9A). In contrast, all three *Cebpg*$^{-/-}$ genotypes exhibited impaired growth. Notably, the double-knockout cells showed no detectable proliferation, and visual inspection of the cultures revealed massive cell death within the first 48 h after plating. This immediate cell death precluded further analysis of *Cebpg*$^{-/-}$; *Cebpb*$^{-/-}$ cells. In addition, *Cebpb* heterozygosity did not rescue the proliferation defect of *Cebpg*$^{-/-}$ cells. These find-

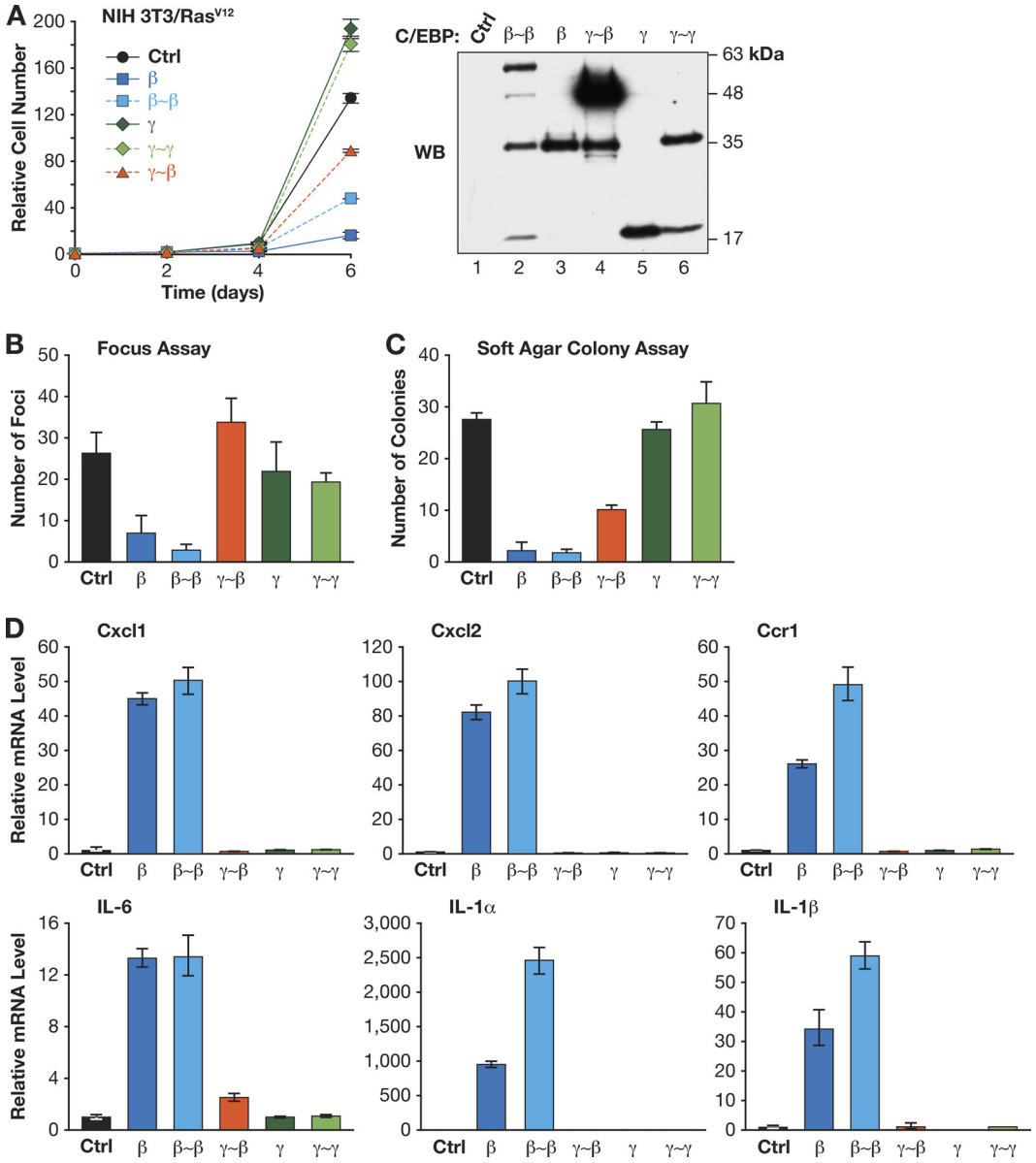

FIG 7 C/EBPβ homodimers inhibit growth and Ras^{V12}-induced transformation in NIH 3T3 cells. (A) Proliferation rates were determined for cells expressing the indicated C/EBP proteins. Right, C/EBP protein levels. The cells were plated for focus assays (B) or soft agar colony growth assays (C). Data are the mean values ± SEM from 3 experiments, each assayed in duplicate. (D) SASP gene expression in 3T3^{RasV12} cells expressing C/EBPβ, C/EBPγ, or linked dimers. Data are the mean values ± SEM from 2 measurements (performed in triplicate) from 2 independent samples.

ings indicate that C/EBPβ provides an essential survival signal in C/EBPγ-deficient cells, but decreasing the *Cebpb* gene dosage to one copy is insufficient to reverse the growth impairment.

We next used RNAi to partially deplete C/EBPβ in *Cebpg*$^{-/-}$ cells, reasoning that reducing C/EBPβ to a level below that of *Cebpb*$^{+/-}$ cells might abrogate senescence without eliciting apoptosis observed in double-knockout MEFs. C/EBPβ knockdown with two independent shRNAs increased the proliferative capacity of *Cebpg*$^{-/-}$ MEFs, as judged by cell densities 7 days after plating (Fig. 9B). C/EBPβ ablation also significantly reduced the proportion of senescent cells (Fig. 9C) and reversed the aberrant expression of SASP genes *Cxcl1* and *Cxcl2* (Fig. 9D). These results indicate that C/EBPβ is required for the premature senescent phenotype of cells lacking C/EBPγ.

If the proproliferative effects of C/EBPγ involve forming heterodimers with C/EBPβ, we anticipated that expression of γ~β-linked dimers would at least partially reverse the growth defect in *Cebpg*$^{-/-}$ MEFs. Indeed, γ~β dimers restored proliferation of *Cebpg*$^{-/-}$ cells as efficiently as C/EBPγ itself (Fig. 10A and B) and also prevented senescence (Fig. 10C). Thus, the presence of C/EBPβ:C/EBPγ heterodimers is critical for maintaining cellular homeostasis and suppressing senescence of MEFs *in vitro*.

C/EBPγ is required for proliferation of hematopoietic cells and human tumor cells. Since C/EBPγ is expressed in most cell types, we asked whether C/EBPγ regulates proliferation of other cells, such as hematopoietic progenitors. *Cebpg*$^{-/-}$ newborn mice reach adulthood on a mixed C57BL/6-129Sv strain background (although perinatal lethality is observed on purebred C57BL/6

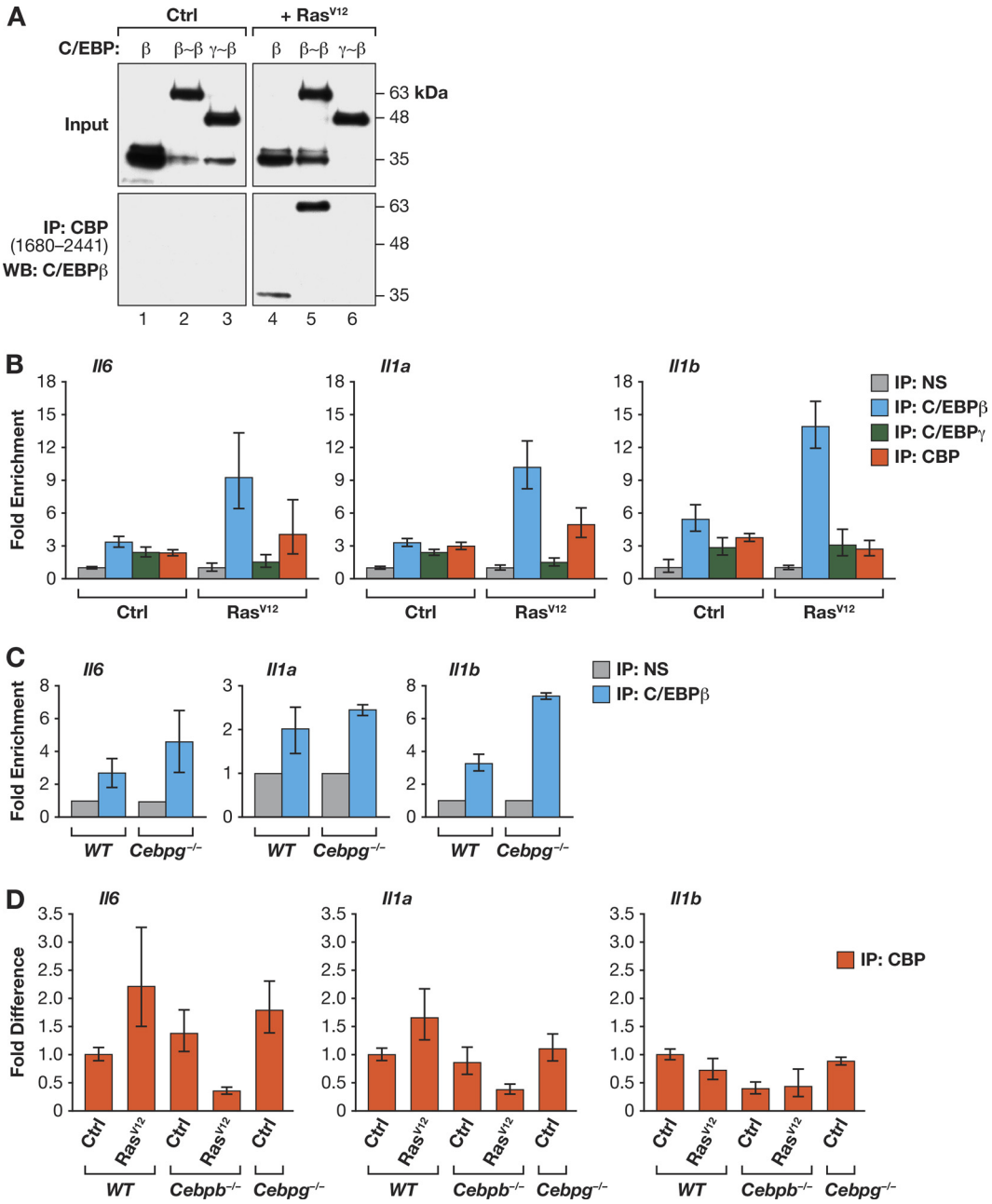

FIG 8 C/EBPβ homodimers recruit the CBP coactivator. (A) C/EBPβ homodimers but not γ~β heterodimers bind to CBP in a Ras^{V12}-dependent manner. C/EBP proteins were coexpressed with a Flag-tagged C-terminal fragment of CBP containing the TAZ2 domain (CBP$_{1680-2441}$) in 293T cells, without or with Ras^{V12}. Cell lysates were immunoprecipitated with Flag antibody and analyzed for C/EBPβ. (B) Association of C/EBPβ, C/EBPγ, and CBP with SASP gene promoters in MEFs. ChIP assays were performed using control and Ras^{V12}-expressing cells; qPCR was performed with primers spanning C/EBP binding sites in the *Il6*, *Il1a*, and *Il1b* promoters (see materials and methods in the supplemental material). Binding was normalized to nonspecific (NS) antibody values. Data are from a representative experiment assayed in triplicate. (C) Increased binding of C/EBPβ to SASP gene promoters in *Cebpg*$^{-/-}$ MEFs. ChIP was performed as described for panel B. (D) Ras^{V12}-induced recruitment of CBP to SASP gene promoters requires C/EBPβ. CBP ChIP was performed on WT, *Cebpb*$^{-/-}$, and *Cebpg*$^{-/-}$ MEFs. For each gene, the values are normalized to CBP binding in WT control cells (without Ras^{V12}). Ras^{V12}-expressing *Cebpg*$^{-/-}$ cells were not included in this experiment since they are undergoing spontaneous senescence, and the objective was to explain increased basal expression of SASP genes in the mutant cells.

and 129Sv backgrounds [16; data to be reported elsewhere]). Therefore, we isolated bone marrow from WT, heterozygous, and homozygous knockout C57BL/6-129Sv animals and analyzed EdU incorporation in the presence of defined growth factors to assess the effect of C/EBPγ deficiency on various hematopoietic lineages (Fig. 11A). Although C/EBPγ loss did not affect the response to M-CSF (macrophages), fewer EdU-positive *Cebpg*$^{-/-}$ cells than in the WT were observed with G-CSF/SCF (granulocytes), GM-CSF/IL-3 (bipotent myeloid progenitors), or SCF/TPO/FLT-3L/IL-3 (early multipotent progenitors). To further

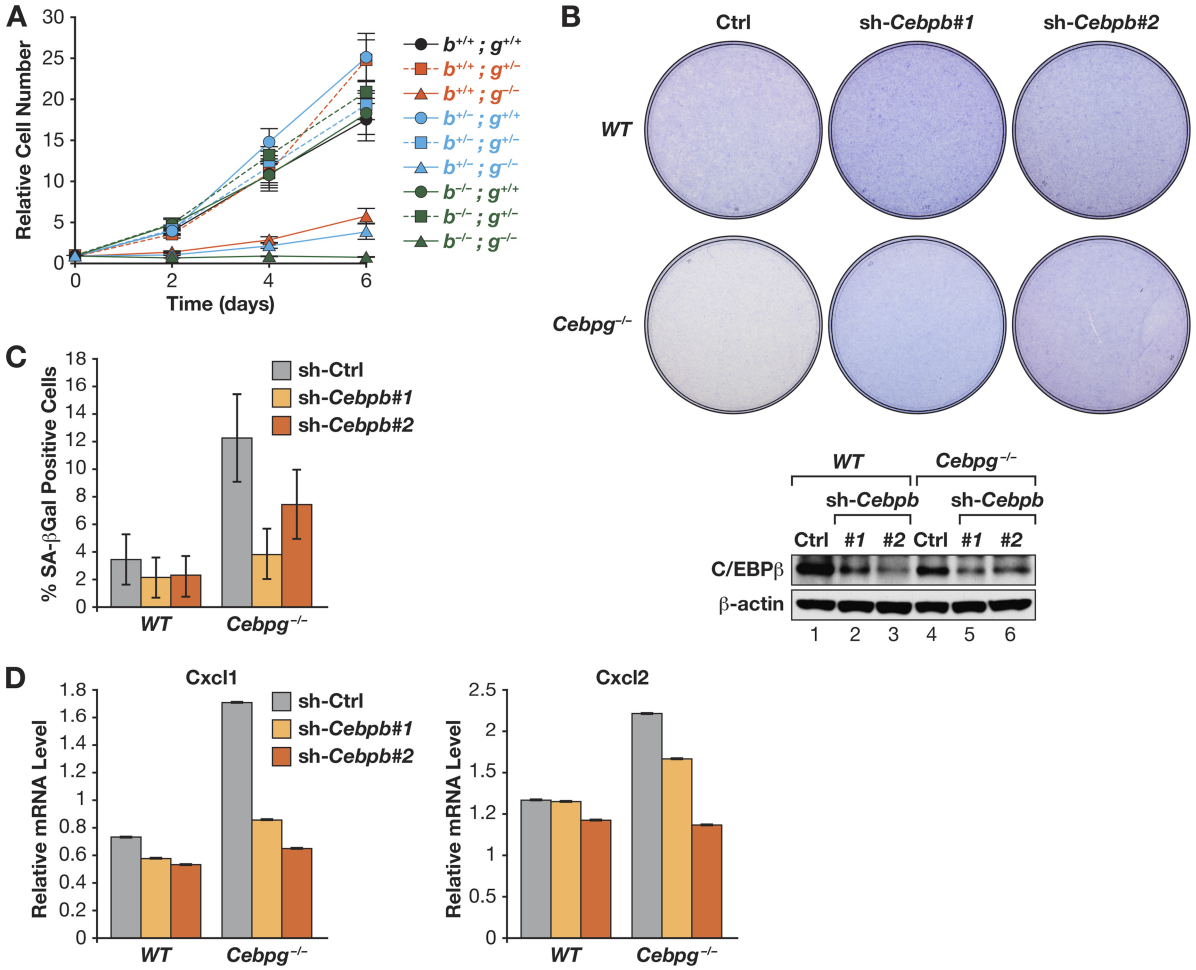

FIG 9 C/EBPβ depletion partially rescues the proliferation defect in *Cebpg*$^{-/-}$ MEFs. (A) Proliferation assays of *Cebpb*; *Cebpg* double-knockout MEFs. MEFs from embryos representing all 9 possible genotypes were seeded at 25,000 cells/well, and proliferation was measured over 6 days. *Cebpb*$^{-/-}$; *Cebpg*$^{-/-}$ cells underwent rapid apoptosis after plating, and nearly all cells died during growth assays. (B) Partial depletion of C/EBPβ restores growth of *Cebpg*$^{-/-}$ MEFs. WT and mutant cells were infected with two different C/EBPβ shRNA retroviruses. Cells were seeded at 10^6 cells/plate, and proliferation was assessed by staining after 7 days. Bottom, C/EBPβ Western blot. (C) C/EBPβ knockdown abrogates the increased senescence seen in *Cebpg*$^{-/-}$ MEFs. SA–β-Gal assays were performed on the cells described for panel B. The data are mean values ± SD (>400 cells were analyzed). (D) Elevated expression of *Cxcl1* and *Cxcl2* in *Cebpg*$^{-/-}$ cells requires C/EBPβ. Expression was analyzed by qPCR; data are the mean values ± SEM from 2 replicate measurements assayed in triplicate.

evaluate this effect, we performed CFU-c assays using the same cytokines (Fig. 11B). In all cases, *Cebpg*$^{-/-}$ cells formed significantly fewer colonies, and intermediate effects were observed for heterozygous cells. Thus, C/EBPγ deficiency impairs S-phase entry and decreases clonogenicity of several hematopoietic lineages and progenitors.

Because most tumor cells divide rapidly, we asked whether C/EBPγ also plays a role in proliferation of cancer cells and disease mortality. We queried the PrognoScan database (26) to identify possible connections between C/EBPγ expression and human malignancies. Thirteen clinical cancer studies showed statistically significant associations between C/EBPγ mRNA levels and clinical endpoints, and in 11 of these studies, higher C/EBPγ expression was correlated with poorer outcomes. An example is shown in Fig. 11C, where C/EBPγ expression in non-small cell lung tumors stratifies patients with decreased probability of relapse-free survival (high C/EBPγ) from those having a more favorable prognosis (low C/EBPγ). These data suggest a growth or survival advantage conferred by elevated C/EBPγ levels in tumor cells. To further explore this possibility, we depleted C/EBPγ in the human lung tumor (alveolar adenocarcinoma) cell line, A549. Ablation of C/EBPγ by two different shRNAs caused a marked (~70%) reduction in colony growth compared to that caused by a control shRNA (Fig. 11D). SA–β-Gal staining also revealed 5- to 8-fold increases in the proportion of senescent cells in the C/EBPγ-depleted populations (Fig. 11E). Therefore, C/EBPγ is required for efficient proliferation and suppression of senescence in lung tumor cells and possibly other cancers.

DISCUSSION

Cellular senescence plays an important role in tumor suppression. Although several cell cycle regulators identified as tumor suppressors are required for OIS, proteins that act as negative regulators of senescence have been less well characterized. Here, we show that C/EBPγ is a growth-promoting transcription factor that suppresses senescence in primary fibroblasts, mainly through its ability to nullify the antiproliferative effects of C/EBPβ.

Despite its ubiquitous expression in mammalian cells (38), the

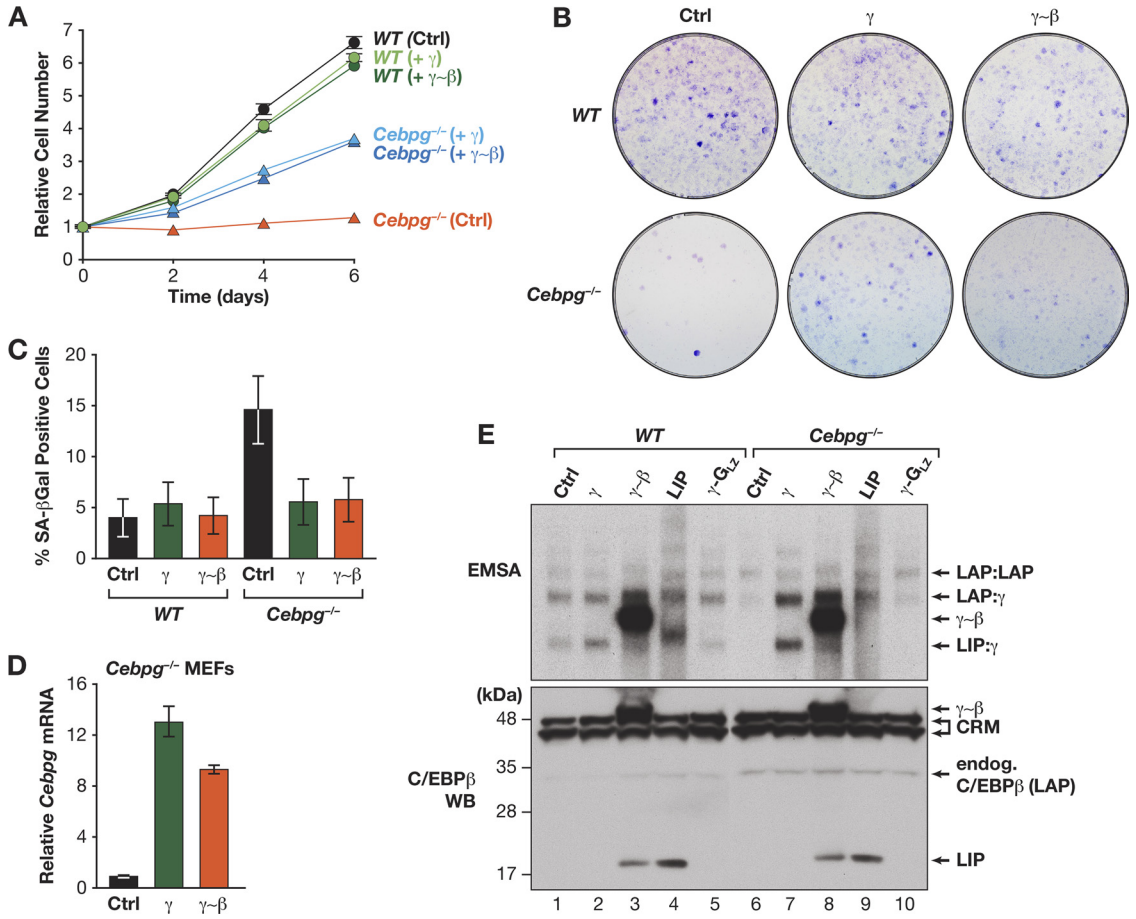

FIG 10 Expression of the γ~β dimer rescues proliferation and inhibits senescence of *Cebpg*$^{-/-}$ MEFs. WT and *Cebpg*$^{-/-}$ cells were infected with retroviruses expressing C/EBPγ or γ~β and analyzed for proliferation (A), colony formation (B), and senescence (SA–β-Gal staining) (C). Proliferation data are mean values ± SD from a representative experiment assayed in triplicate. (D) Ectopic C/EBPγ and γ~β expression in *Cebpg*$^{-/-}$ MEFs. The graph shows *Cebpg* reverse transcription qPCR assays of RNA from retrovirally infected *Cebpg*$^{-/-}$ cells. A weak signal is observed in control *Cebpg*$^{-/-}$ cells because the primers span the *Neo* insert in the knockout allele (16). (E) Ectopic C/EBP protein expression in WT and *Cebpg*$^{-/-}$ MEFs. Top, EMSA of nuclear extracts from the cells described for panel D and for Fig. 5C. LIP DNA-binding activity is not observed in *Cebpg*$^{-/-}$ cells (lane 9), supporting observations from our laboratory that LIP is autoinhibited (25) and can be activated by coexpression of C/EBPγ (unpublished data). Bottom, C/EBPβ Western blot (WB) of the same extracts. The LIP species detected in lanes 3 and 8 is apparently a proteolytic product from the γ~β dimer. CRM, cross-reacting material.

regulatory functions of C/EBPγ have not been characterized. C/EBPγ primarily forms heterodimers with other C/EBP proteins (12, 39). This is consistent with structural predictions indicating that C/EBPγ homodimers are unstable due to repulsive electrostatic interactions between its paired leucine zipper helices (15). Thus, C/EBPγ monomers are available to heterodimerize with other bZIP partners. C/EBPγ lacks an identifiable transactivation domain, and its principal role appears to be as a transdominant inhibitor by heterodimerizing with other C/EBPs (12, 13). However, in some contexts, C/EBPγ may also positively regulate transcription, such as in lipopolysaccharide (LPS)-induced activation of the *Il6* and *Il8* promoters in B lymphoblasts (18).

We found that C/EBPγ suppresses basal expression of SASP genes in primary MEFs by dimerizing with C/EBPβ and inhibiting its transcriptional activity. C/EBPγ deficiency caused a marked increase in C/EBPβ homodimers, which coincided with reduced cell proliferation, increased senescence, and activation of SASP genes. Knockdown of C/EBPβ partially rescued this phenotype, supporting the idea that C/EBPβ homodimers induce growth arrest and activate proinflammatory genes. Accordingly, expression of tethered β~β homodimers inhibited proliferation and stimulated SASP gene expression, while γ~β dimers lacked these activities. γ~β restored growth and inhibited senescence in *Cebpg*$^{-/-}$ cells, indicating that the β:γ heterodimers play a critical role in maintaining cellular homeostasis. β~β but not γ~β dimers bound stably to CBP in a Ras^{V12}-dependent manner, consistent with previous findings showing that the interaction of C/EBPβ with p300/CBP is stimulated by Ras (25, 36). We previously identified several protein interaction motifs in the C/EBPβ TAD and regulatory domains that mediate autoinhibition and p300/CBP binding (25). Ras-induced posttranslational modifications that derepress C/EBPβ occur at nearby sites, and these modified residues may also stabilize interactions with coactivators. This could explain why the C/EBPβ-p300/CBP association depends on Ras signaling, which was observed even for tethered β~β homodimers that do not require Ras for dimerization.

A model for our findings is depicted in Fig. 11F. In the absence of activating signals such as Ras^{V12}, C/EBPβ remains predominantly in heterodimeric form with C/EBPγ. Heterodimers appear to be permissive for, or actively promote, cell proliferation and

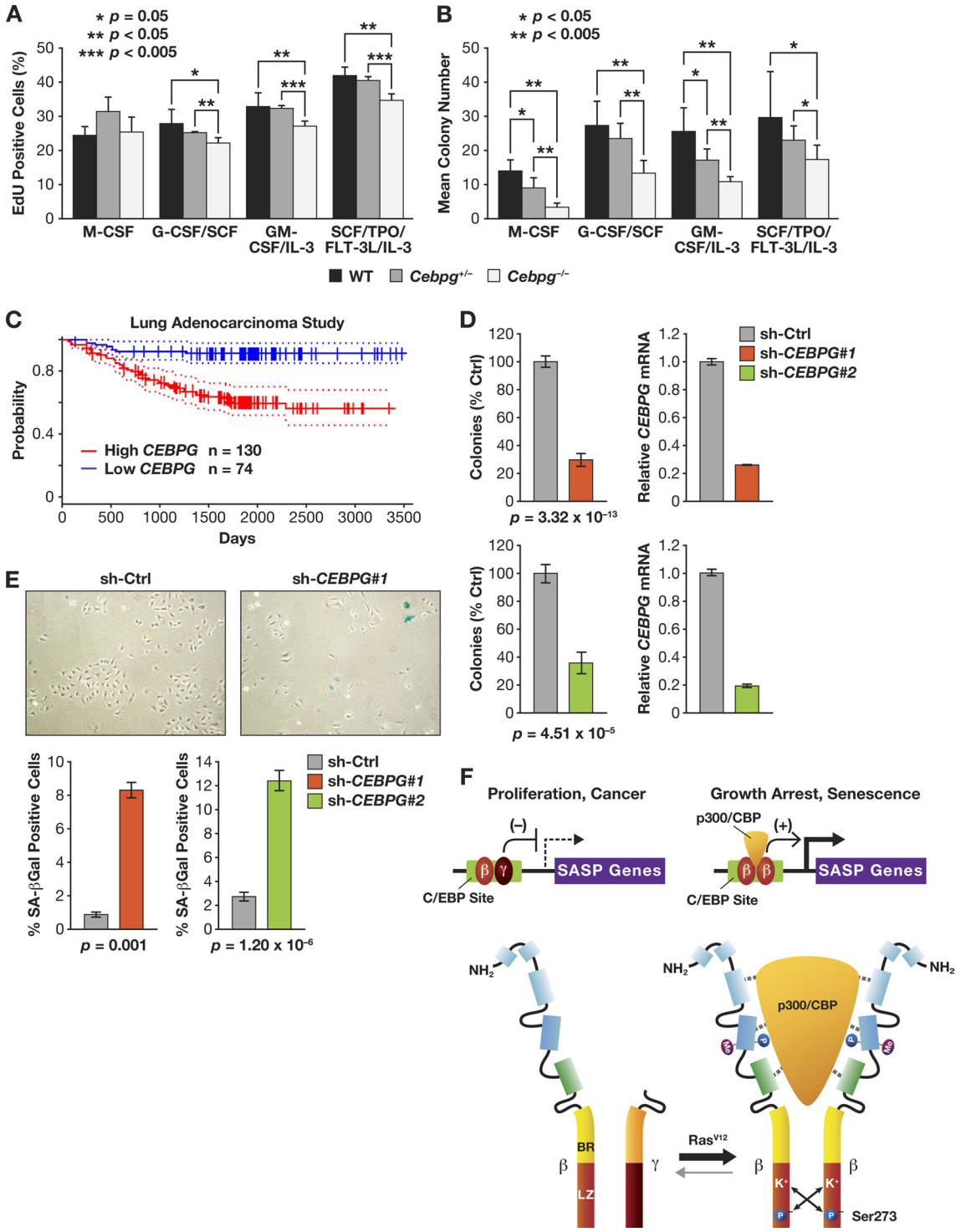

FIG 11 C/EBPγ is required for proliferation of murine hematopoietic cells and human cancer cells. (A, B) Cell proliferation and CFU-c assays of WT and *Cebpg*$^{-/-}$ bone marrow cells. Bone marrow was isolated from adult mice on a mixed C57BL/6-129Sv background. The cells were incubated with the indicated combinations of hematopoietic growth factors and evaluated for proliferation (EdU incorporation assays) (A) and colony growth (1.5×10^4 cells/plate) (B). (C) C/EBPγ expression is negatively associated with relapse-free survival of lung adenocarcinoma patients. Graph shows Kaplan-Meier relapse-free survival from a study of lung adenocarcinoma patients (47) stratified according to high ($n = 130$) and low ($n = 74$) *CEBPG* expression in tumors. Dotted lines indicate 95% confidence intervals. Meta-analysis of microarray data are from PrognoScan (26). (D) C/EBPγ depletion impairs proliferation of human A549 lung adenocarcinoma cells. C/EBPγ was ablated by two independent shRNAs (1 and 2), and colony growth was analyzed. Data are the mean values ± SEM from 2 experiments. C/EBPγ mRNA levels are shown in graphs on the right. (E) Increased senescence in C/EBPγ-depleted A549 cells. Four days after plating, cells were stained for SA–β-Gal, and senescent cells were visualized (upper panels) and counted (bottom panels). Data are mean values ± SEM from 2 experiments. (F) Differential regulatory properties of C/EBPβ homo- and heterodimers. In proliferating cells and in the absence of an activating signal such as oncogenic Ras, C/EBPβ occurs predominantly as a heterodimer with C/EBPγ. β:γ heterodimers bind to target C/EBP sites in SASP gene promoters but are transcriptionally inactive. In cells undergoing Ras-induced senescence, $p90^{RSK}$-mediated phosphorylation on Ser273 in the C/EBPβ leucine zipper stabilizes the LZ interaction and promotes formation of β:β homodimers (15). Activated homodimers are capable of binding p300/CBP, inducing cell cycle arrest, and activating transcription of SASP genes. In contrast, β:γ heterodimers do not recruit p300/CBP and promote cell proliferation and cancer.

cancer. In the presence of Ras^{V12}, C/EBPβ becomes phosphorylated on Ser273, which stabilizes LZ interactions and drives homodimer formation (15). Activated homodimers contain additional modifications that facilitate association with p300/CBP, and this complex induces cell cycle arrest and transcription of SASP genes. A key function of C/EBPγ is to prevent C/EBPβ homodimerization, thereby suppressing senescence and expression of inflammatory mediators until an appropriate signal, such as oncogenic stress, occurs. As newborn C57BL/6 C/EBPγ-deficient mice die within 48 h postnatally (16), future studies will be aimed at determining whether increased inflammation in a critical organ underlies this phenotype.

This model prompts the question of how tumor cells with an activated Ras-Raf-MEK1/2-ERK1/2 pathway evade the cytostatic effects of homodimeric C/EBPβ. We have reported that disruption of RB:E2F renders MEFs insensitive to growth arrest by ectopic C/EBPβ (11). In addition, loss of $p19^{Arf}$ in immortalized murine fibroblasts (e.g., NIH 3T3 cells) causes downregulation of *Cebpb* gene transcription upon expression of oncogenic Ras (35). Ras^{V12}-mediated silencing of the LAP* isoform was also observed in human mammary epithelial cells and involves increased protein degradation (40). Finally, we recently found that the *Cebpb* 3′ untranslated region (3′UTR) inhibits Ras^{V12}-induced posttranslational activation of C/EBPβ in immortalized and transformed cells, but not in primary cells, through an mRNA localization mechanism (8). 3′UTR inhibition maintains C/EBPβ as a heterodimer with C/EBPγ even in the face of sustained Ras signaling. Thus, several mechanisms operate in tumor cells to suppress C/EBPβ's cytostatic activity.

In addition to its role in senescence and tumor suppression, C/EBPβ can promote tumorigenesis through both cell autonomous and nonautonomous mechanisms (29, 41–44). The fact that high C/EBPγ levels are associated with malignancy of several human cancers suggests that C/EBPγ dimerization with C/EBPβ or other bZIP partners promotes tumor cell growth or metastasis. In this regard, a recent study found increased C/EBPγ expression in a subset of acute myeloid leukemias lacking C/EBPα (45). This work showed that C/EBPα negatively regulates C/EBPγ expression in the myeloid lineage, and ablation of C/EBPγ in C/EBPα-deficient AML cells induced granulocytic differentiation. These observations support our findings that C/EBPγ has proliferative and prooncogenic functions.

Interestingly, we found that $Cebpg^{-/-}$; $Cebpb^{-/-}$ MEFs underwent rapid apoptosis in culture. Because neither single mutant caused severe cell death, C/EBPβ and C/EBPγ may have partially redundant functions in promoting cell survival. Furthermore, the apoptotic phenotype of $Cebpg^{-/-}$; $Cebpb^{-/-}$ MEFs results from *in vitro* culture conditions, as E13.5 double-mutant embryos showed no gross defects. Similarly, $Cebpg^{-/-}$ embryos did not display obvious abnormalities, whereas cultured fibroblasts derived from them proliferate very poorly. Stresses associated with *in vitro* cell culture, such as exposure to an oxygenated environment and continuous stimulation by serum growth factors, can accelerate cellular senescence (46). Thus, C/EBPγ may function mainly in the context of cellular stresses that activate C/EBPβ and are normally not encountered in a physiological setting. In this view, C/EBPγ provides a buffer to constrain C/EBPβ activity until stress signals reach a threshold intensity, at which point C/EBPβ becomes strongly activated and induces growth arrest or senescence.

ACKNOWLEDGMENTS

We thank Tsuneyasu Kaisho for providing the $Cebpg^{+/-}$ mice, Philipp Kaldis for Cdk and cyclin antibodies and oncoprotein expression vectors, Angie Hackley and Karen Saylor for animal breeding, genotyping, and assistance with preparation of MEFs, and Jiro Wada and Al Kane (Scientific Publications, Graphics & Media, SAIC—Frederick, Inc.) for preparation of figures.

This research was supported by the Intramural Research Program of the NIH, National Cancer Institute, Center for Cancer Research.

REFERENCES

1. **Campisi J.** 2005. Senescent cells, tumor suppression, and organismal aging: good citizens, bad neighbors. Cell **120:**513–522.
2. **Kuilman T, Michaloglou C, Mooi WJ, Peeper DS.** 2010. The essence of senescence. Genes Dev. **24:**2463–2479.
3. **Lowe SW, Cepero E, Evan G.** 2004. Intrinsic tumour suppression. Nature **432:**307–315.
4. **Coppe J-P, Desprez P-Y, Krtolica A, Campisi J.** 2010. The senescence-associated secretory phenotype: the dark side of tumor suppression. Annu. Rev. Pathol. **5:**99–118.
5. **Kang TW, Yevsa T, Woller N, Hoenicke L, Wuestefeld T, Dauch D, Hohmeyer A, Gereke M, Rudalska R, Potapova A, Iken M, Vucur M, Weiss S, Heikenwalder M, Khan S, Gil J, Bruder D, Manns M, Schirmacher P, Tacke F, Ott M, Luedde T, Longerich T, Kubicka S, Zender L.** 2011. Senescence surveillance of pre-malignant hepatocytes limits liver cancer development. Nature **479:**547–551.
6. **Acosta JC, O'Loghlen A, Banito A, Guijarro MV, Augert A, Raguz S, Fumagalli M, Da Costa M, Brown C, Popov N, Takatsu Y, Melamed J, d'Adda di Fagagna F, Bernard D, Hernando E, Gil J.** 2008. Chemokine signaling via the CXCR2 receptor reinforces senescence. Cell **133:**1006–1018.
7. **Kuilman T, Michaloglou C, Vredeveld LC, Douma S, van Doorn R, Desmet CJ, Aarden LA, Mooi WJ, Peeper DS.** 2008. Oncogene-induced senescence relayed by an interleukin-dependent inflammatory network. Cell **133:**1019–1031.
8. **Basu SK, Malik R, Huggins CJ, Lee S, Sebastian T, Sakchaisri K, Quinones OA, Alvord WG, Johnson PF.** 2011. 3′UTR elements inhibit Ras-induced C/EBPbeta post-translational activation and senescence in tumour cells. EMBO J. **30:**3714–3728.
9. **Chien Y, Scuoppo C, Wang X, Fang X, Balgley B, Bolden JE, Premsrirut P, Luo W, Chicas A, Lee CS, Kogan SC, Lowe SW.** 2011. Control of the senescence-associated secretory phenotype by NF-kappaB promotes senescence and enhances chemosensitivity. Genes Dev. **25:**2125–2136.
10. **Rodier F, Coppe JP, Patil CK, Hoeijmakers WA, Munoz DP, Raza SR, Freund A, Campeau E, Davalos AR, Campisi J.** 2009. Persistent DNA damage signalling triggers senescence-associated inflammatory cytokine secretion. Nat. Cell Biol. **11:**973–979.
11. **Sebastian T, Malik R, Thomas S, Sage J, Johnson PF.** 2005. C/EBPbeta cooperates with RB:E2F to implement Ras(V12)-induced cellular senescence. EMBO J. **24:**3301–3312.
12. **Parkin SE, Baer M, Copeland TD, Schwartz RC, Johnson PF.** 2002. Regulation of CCAAT/enhancer-binding protein (C/EBP) activator proteins by heterodimerization with C/EBPgamma (Ig/EBP). J. Biol. Chem. **277:**23563–23572.
13. **Cooper C, Henderson A, Artandi S, Avitahl N, Calame K.** 1995. Ig/EBP (C/EBP gamma) is a transdominant negative inhibitor of C/EBP family transcriptional activators. Nucleic Acids Res. **23:**4371–4377.
14. **Thomassin H, Hamel D, Bernier D, Guertin M, Belanger L.** 1992. Molecular cloning of two C/EBP-related proteins that bind to the promoter and the enhancer of the alpha 1-fetoprotein gene. Further analysis of C/EBP beta and C/EBP gamma. Nucleic Acids Res. **20:**3091–3098.
15. **Lee S, Shuman JD, Guszczynski T, Sakchaisri K, Sebastian T, Copeland TD, Miller M, Cohen MS, Taunton J, Smart RC, Xiao Z, Yu L-R, Veenstra TD, Johnson PF.** 2010. RSK-mediated phosphorylation in the C/EBP{beta} leucine zipper regulates DNA binding, dimerization, and growth arrest activity. Mol. Cell. Biol. **30:**2621–2635.
16. **Kaisho T, Tsutsui H, Tanaka T, Tsujimura T, Takeda K, Kawai T, Yoshida N, Nakanishi K, Akira S.** 1999. Impairment of natural killer cytotoxic activity and interferon gamma production in CCAAT/enhancer binding protein gamma-deficient mice. J. Exp. Med. **190:**1573–1582.
17. **Bakiri L, Matsuo K, Wisniewska M, Wagner EF, Yaniv M.** 2002.

Promoter specificity and biological activity of tethered AP-1 dimers. Mol. Cell. Biol. **22:**4952–4964.
18. **Gao H, Parkin S, Johnson PF, Schwartz RC.** 2002. C/EBP gamma has a stimulatory role on the IL-6 and IL-8 promoters. J. Biol. Chem. **277:**38827–38837.
19. **Chen Z, Torrens JI, Anand A, Spiegelman BM, Friedman JM.** 2005. Krox20 stimulates adipogenesis via C/EBPbeta-dependent and -independent mechanisms. Cell Metab. **1:**93–106.
20. **Kajimura S, Seale P, Kubota K, Lunsford E, Frangioni JV, Gygi SP, Spiegelman BM.** 2009. Initiation of myoblast to brown fat switch by a PRDM16-C/EBP-beta transcriptional complex. Nature **460:**1154–1158.
21. **Reuter JS, Mathews DH.** 2010. RNAstructure: software for RNA secondary structure prediction and analysis. BMC Bioinformatics **11:**129.
22. **Todaro GJ, Green H.** 1963. Quantitative studies of the growth of mouse embryo cells in culture and their development into established lines. J. Cell Biol. **17:**299–313.
23. **Berthet C, Aleem E, Coppola V, Tessarollo L, Kaldis P.** 2003. Cdk2 knockout mice are viable. Curr. Biol. **13:**1775–1785.
24. **Baer M, Johnson PF.** 2000. Generation of truncated C/EBPβ isoforms by *in vitro* proteolysis. J. Biol. Chem. **275:**26582–26590.
25. **Lee S, Miller M, Shuman JD, Johnson PF.** 2010. CCAAT/enhancer-binding protein beta DNA binding is auto-inhibited by multiple elements that also mediate association with p300/CREB-binding protein (CBP). J. Biol. Chem. **285:**21399–21410.
26. **Mizuno H, Kitada K, Nakai K, Sarai A.** 2009. PrognoScan: a new database for meta-analysis of the prognostic value of genes. BMC Med. Genomics **2:**18.
27. **Gentleman R, Carey V, Bates D, Bolstad B, Dettling M, Dudoit S, Ellis B, Gautier L, Ge Y, Gentry J, Hornik K, Hothorn T, Huber W, Iacus S, Irizarry R, Leisch F, Li C, Maechler M, Rossini A, Sawitzki G, Smith C, Smyth G, Tierney L, Yang J, Zhang J.** 2004. Bioconductor: open software development for computational biology and bioinformatics. Genome Biol. **5:**R80.
28. **R Development Core Team.** 2010. R: a language and environment for statistical computing. R Foundation for Statistical Computing, Vienna, Austria. http://www.R-project.org.
29. **Sebastian T, Johnson PF.** 2006. Stop and go: anti-proliferative and mitogenic functions of the transcription factor C/EBPbeta. Cell Cycle **5:**953–957.
30. **Malek NP, Sundberg H, McGrew S, Nakayama K, Kyriakides TR, Roberts JM.** 2001. A mouse knock-in model exposes sequential proteolytic pathways that regulate p27Kip1 in G_1 and S phase. Nature **413:**323–327.
31. **Bartek J, Hodny Z, Lukas J.** 2008. Cytokine loops driving senescence. Nat. Cell Biol. **10:**887–889.
32. **Jun JI, Lau LF.** 2010. Cellular senescence controls fibrosis in wound healing. Aging **2:**627–631.
33. **Krizhanovsky V, Yon M, Dickins RA, Hearn S, Simon J, Miething C, Yee H, Zender L, Lowe SW.** 2008. Senescence of activated stellate cells limits liver fibrosis. Cell **134:**657–667.
34. **Descombes P, Schibler U.** 1991. A liver-enriched transcriptional activator protein, LAP, and a transcriptional inhibitory protein, LIP, are translated from the same mRNA. Cell **67:**569–579.
35. **Sebastian T, Johnson PF.** 2009. RasV12-mediated down-regulation of CCAAT/enhancer binding protein {beta} in immortalized fibroblasts requires loss of p19Arf and facilitates bypass of oncogene-induced senescence. Cancer Res. **69:**2588–2598.
36. **Oelgeschlager M, Janknecht R, Krieg J, Schreek S, Luscher B.** 1996. Interaction of the co-activator CBP with Myb proteins: effects on Myb-specific transactivation and on the cooperativity with NF-M. EMBO J. **15:**2771–2780.
37. **Akira S, Isshiki H, Sugita T, Tanabe O, Kinoshita S, Nishio Y, Nakajima T, Hirano T, Kishimoto T.** 1990. A nuclear factor for IL-6 expression (NF-IL6) is a member of a C/EBP family. EMBO J. **9:**1897–1906.
38. **Roman C, Platero JS, Shuman J, Calame K.** 1990. Ig/EBP-1: a ubiquitously expressed immunoglobulin enhancer binding protein that is similar to C/EBP and heterodimerizes with C/EBP. Genes Dev. **4:**1404–1415.
39. **Newman JR, Keating AE.** 2003. Comprehensive identification of human bZIP interactions with coiled-coil arrays. Science **300:**2097–2101.
40. **Atwood AA, Sealy L.** 2010. Regulation of C/EBPbeta1 by Ras in mammary epithelial cells and the role of C/EBPbeta1 in oncogene-induced senescence. Oncogene **29:**6004–6015.
41. **Staiger J, Lueben MJ, Berrigan D, Malik R, Perkins SN, Hursting SD, Johnson PF.** 2009. C/EBPbeta regulates body composition, energy balance-related hormones and tumor growth. Carcinogenesis **30:**832–840.
42. **Sterneck E, Zhu S, Ramirez A, Jorcano JL, Smart RC.** 2006. Conditional ablation of C/EBP beta demonstrates its keratinocyte-specific requirement for cell survival and mouse skin tumorigenesis. Oncogene **25:**1272–1276.
43. **Zahnow CA.** 2009. CCAAT/enhancer-binding protein beta: its role in breast cancer and associations with receptor tyrosine kinases. Expert Rev. Mol. Med. **11:**e12.
44. **Zhu S, Yoon K, Sterneck E, Johnson PF, Smart RC.** 2002. CCAAT/enhancer binding protein-beta is a mediator of keratinocyte survival and skin tumorigenesis involving oncogenic Ras signaling. Proc. Natl. Acad. Sci. U. S. A. **99:**207–212.
45. **Alberich-Jorda M, Wouters B, Balastik M, Shapiro-Koss C, Zhang H, Di Ruscio A, Radomska HS, Ebralidze AK, Amabile G, Ye M, Zhang J, Lowers I, Avellino R, Melnick A, Figueroa ME, Valk PJ, Delwel R, Tenen DG.** 2013. C/EBPgamma deregulation results in differentiation arrest in acute myeloid leukemia. J. Clin. Invest. **122:**4490–4504.
46. **Sherr CJ, DePinho RA.** 2000. Cellular senescence: mitotic clock or culture shock? Cell **102:**407–410.
47. **Okayama H, Kohno T, Ishii Y, Shimada Y, Shiraishi K, Iwakawa R, Furuta K, Tsuta K, Shibata T, Yamamoto S, Watanabe S, Sakamoto H, Kumamoto K, Takenoshita S, Gotoh N, Mizuno H, Sarai A, Kawano S, Yamaguchi R, Miyano S, Yokota J.** 2012. Identification of genes upregulated in ALK-positive and EGFR/KRAS/ALK-negative lung adenocarcinomas. Cancer Res. **72:**100–111.